

## MODELLING AND SIMULATION OF THE IMPURITY DIFFUSION AND RELATED PHENOMENA IN SILICON AND POLYSILICON SYSTEMS IN MICROFABRICATION AND MICROMACHINING TECHNOLOGIES

Florin GAISEANU

*Abstract* - In this paper there are presented our results concerning the modelling and simulation diffusion of the boron, phosphorus, antimony, arsenic as doping impurities in silicon and polysilicon layers and gold diffusion as a recombination centre in silicon and its influence on the forward characteristic of the p-n junction, as well as some related phenomena like the generation of the misfit dislocations induced by the doping impurities and the gettering process of metallic impurities, with application in the microfabrication technologies. The results on the boron diffusion were used in the simulation of the self-limited etching process of silicon boron doped layers for the bulk micromachining fabrication and the powerful methods as XTEM and SIMS were used for the characterizations of the polysilicon layers, allowing to propose a doping – restructuring mechanism of polysilicon during the phosphorus diffusion in the surface micromachining technology for the thin membrane achievement.

**Keywords:** Impurity Diffusion, Modelling and Simulation, Misfit Dislocations, Gettering, Etching, Silicon and Polysilicon, Doping-Restructuring Model, Micromachining and Microfabrication

### 1. Introduction

The knowledge of the material properties of the semiconductor in the delimited specific regions of the semiconductor both before and after processing is one of the fundamental tasks for the achievement of the microelectronic and microsystem devices in order to accurately design their configuration and to control on this way the desired useful parameters [1]. The fulfilment of these fundamental requirements explains the considerable efforts to investigate the material properties at the atomic scale [2] and to formulate in physical and mathematical terms the intimate atomic processes in the semiconductor lattice [3].

In this paper there are presented our contributions to the description of the atomic diffusion in silicon of boron as a *p*-type impurity in silicon and of phosphorus, antimony and arsenic as *n*-type impurities, by using conventional (thermo-chemical) and non-conventional (doped polysilicon, multilayer systems, implantation, laser - assisted annealing) techniques, as well as the gold diffusion and its influence on the forward characteristic of p-n junction and the gettering phenomena induced by the diffusion in silicon wafers. As a related process during the phosphorus and boron diffusion in silicon at high concentrations, the generation of the misfit dislocations, defined in terms of the critical conditions and the corresponding variation of the characteristic parameters (critical diffusion time and temperature) is calculated and expressed in analytical form.

There are presented also the main investigations results concerning the chemical etching of boron doped layers and doping – restructuring of polysilicon layers during the phosphorus diffusion, as a key processes in bulk and surface micromachining technology respectively, for the fabrication of the silicon membranes.

## **2. Modeling and simulation of the impurity diffusion by thermo-chemical method**

The thermo-chemical method is the most frequently used for the silicon doping and is performed under a constant temperature maintained in the diffusion tube of the furnace and a permanent contact between the silicon wafer surface and the chemical doping agent, which is usually a  $BBr_3$  liquid source or boron nitride (BN) solid source for the p-type doping and a liquid  $POCl_3$  source for the n-type doping. The knowledge of the variation with the depth of the impurity is essential for the design and fabrication of the semiconductor devices, so that it is a very important to determine not only the concentration distribution with the depth after the diffusion, but also if the entire quantity of the doping impurity is fully electrical active.

### **2.1. Experimental determination of electrically active and inactive boron and phosphorus profiles in silicon**

For this purpose, it was used the sheet resistivity method, consisting in the measurement of the sheet resistivity with the four point method after successive removal of thin silicon doped layers, by using a mixture of HF and  $K_2Cr_2O_7$  and a mixture of HF,  $HNO_3$  and  $CH_3COOH$  to determine the electrically active impurity profile for phosphorus and boron respectively and two chemical method to determine the full impurity profile, electrically active and inactive of phosphorus [4] and boron [5, 6] in silicon. It was reported for the first time in the literature the use of these chemical methods for the impurity profile determination: the spectrographic emission dosing for the determination of the total boron concentration profile after diffusion in silicon and the spectrophotometric dosing method for the determination of the total phosphorus diffusion profile. The spectrographic emission dosing consists in the determination of the emission spectrum of the chemical solution step, submitted to a suitable preparation after each etching step, and a comparative analysis of the spectral lines. The spectrophotometric method for the phosphorus dosing is similar with the spectrographic emission dosing, but the final determinations are made by a photospectrometer.

The results are presented in Fig.1 (a) and (b), where are shown the boron diffusion profile after diffusion from a BN source at the temperature  $T=1100^\circ C$  for 120 min and the phosphorus diffusion profile after the diffusion from a liquid  $POCl_3$

source at  $T = 1000^{\circ}\text{C}$  for 30 min respectively, in comparison with the theoretical profile (erfc type) deduced from the diffusion equation if a diffusion coefficient independent of concentration would operate in the two cases. As it can be seen from Fig.1, both the boron and phosphorus profile is very different of the theoretical profile. Another conclusion from Fig. 1. is that the entire quantity of the boron diffused is electrically active, while an important quantity of phosphorus is electrically inactive after the diffusion, so our next objective of the investigation was to try to describe correctly this specific behavior, as it is presented in the following sections.

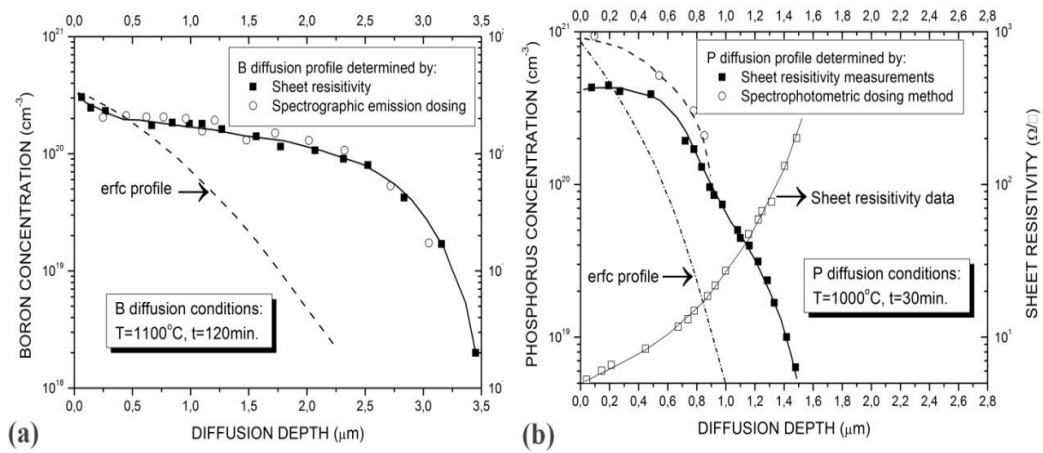


**Fig. 1.** Experimentally determined (a) boron diffusion profile and (b) phosphorus diffusion profile by an electrically and chemical method and the comparison with the theoretical ERFC profile.

## 2.2. Modeling and simulation of boron diffusion in silicon

Representing the distribution along the depth  $x$  of the boron concentration  $C$  in silicon after the diffusion from infinite source as so called universal profile, i.e.  $C/C_0$  ( $C_0$  being the surface value of  $C$ ) as a function of a quantity  $x/2\sqrt{Dot}$ , where  $Do$  is the surface value of the diffusion coefficient and  $t$  the diffusion time, we shown for the first time [7] that this one can be suitably described on the concentration range  $C > n_i$  (extrinsic region), where  $n_i$  represents the intrinsic carrier concentration, by a solution of the diffusion equation

$$\frac{\partial C}{\partial t} = \frac{\partial}{\partial x}[D(C)\frac{\partial C}{\partial x}] \quad (1)$$

with a diffusion coefficient  $D$  depending on the boron concentration as:

$$D = D_0(C/C_0)^{1/2} \quad (2)$$

instead of a simple linear dependence, which would be typical for diffusion by a vacancy mechanism [8], as it can be seen in Fig. 2. The depth  $x_l$  in Fig. 2 (a)

corresponds to a concentration of  $10^{18} \text{ cm}^{-3}$ , taken as a reference limit value in order to analyse the experimental data only on the extrinsic range.

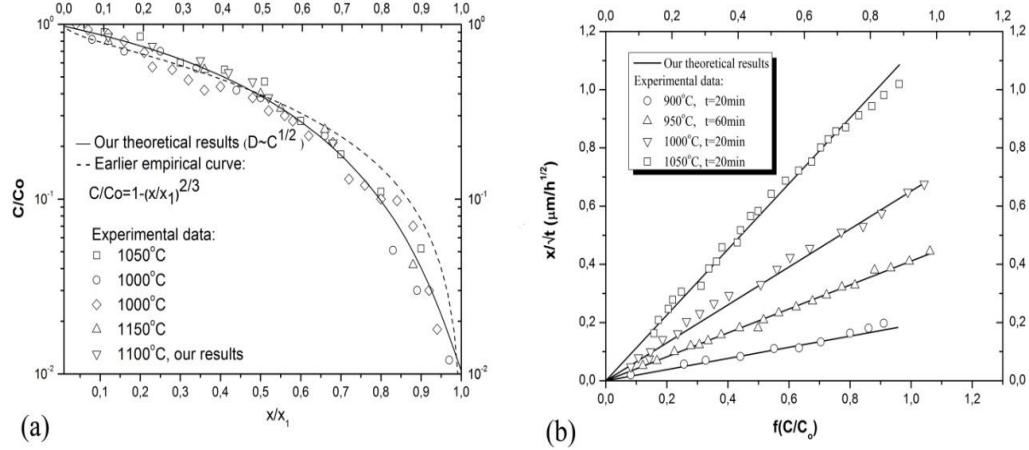


**Fig. 2.** Boron diffusion profile represented as:

- (a) normalized quantity  $C/Co$  vs.  $x/x_1$  (universal profile) [7];  
 (b) variation of  $x/\sqrt{t}$  vs.  $f(C/Co)$ , which is the right side of the solution of the diffusion equation (rel. (3)), depending only on  $C$  and  $Co$  [9] (the experimental data were collected from [10]).

We deduced [11] a proper solution of the diffusion equation (1) with the diffusion coefficient described by the relation (2) as a following polynomial form:

$$x/2.33\sqrt{Dot} = 1 - 0.737(C/Co)^{1/2} - 0.181(C/Co) - 0.082(C/Co)^{3/2} \quad (3)$$

which express the diffusion depth as a function of the impurity concentration with accuracy better than 3%. A very good agreement between the experimental data and our theoretical results can be noticed from Fig. 2., allowing the accurate simulation of the boron diffusion profile by means of rel. (3) on the extrinsic range. Moreover, the form (3) represented by  $x/\sqrt{t}$  vs.  $f(C/Co)$  as a right line in Fig. 2 (b) permits an accurate evaluation of the surface diffusion coefficient  $Do$  and of the surface concentration  $Co$  by an adequate extraction procedure of the interest parameters [9], resulting:

$$Do = 0.4648 \exp(-3.08 \text{ eV}/kT) \quad (4)$$

and 
$$Co = 1.43 \times 10^{22} \exp(-0.44 \text{ eV}/kT) \quad (5)$$

over the experimental data on the range 900°C - 1050°C collected from [10].

By using relation (3) it was possible also to express the boron atom amount

$$Q(t, T) = 0.9 Co \sqrt{Dot} \quad (6)$$

diffused in silicon from a  $BBr_3$  source [11, 12], in agreement with the experimental data from [12] (Fig. 3 (a)).

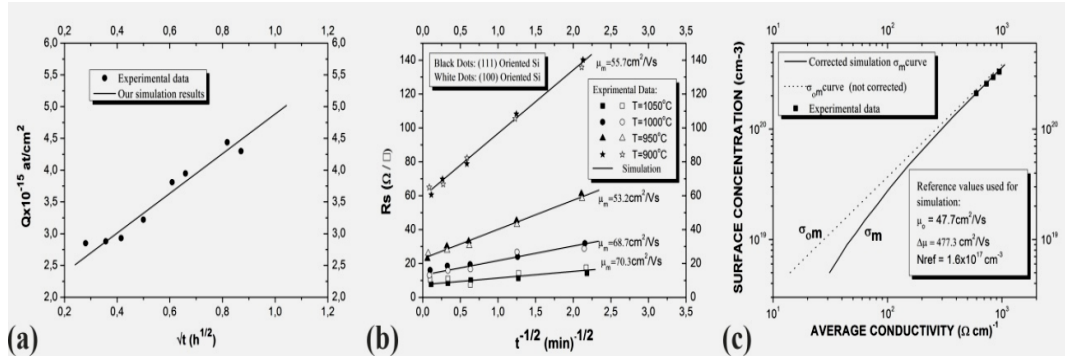


**Fig. 3.** (a) Simulated boron amount as a function of the square root of the diffusion time compared with experimental data [12]. Simulated  $R_s$  as depending on the reverse of the square root of the diffusion time, compared with experimental data from [10]. (b) Our theoretical curve  $C_0$  vs. average conductivity  $\sigma_m$  compared with the curve  $C_0$  vs.  $\sigma_{om}$  earlier proposed [8] and with experimental data [10].

Relation (3) permits to calculate also in an explicit way the sheet resistivity  $R_s$  of the boron doped silicon layers [9], which is a material parameter measurable by using the four point method. This is practically one of the most commonly used parameter not only to control the doping after diffusion but also to design the silicon semiconductor devices, so that its predictability as a function of the diffusion conditions is of major practical interest in the silicon semiconductor technology. Taking into account rel. (3),  $R_s$  was calculated on the high concentration range [13] as  $R_s = [qCo\mu_m(Dot)^{1/2}]^{-1}$ , where  $\mu_m$  represents an average value of the hole mobility on the variation range of concentration, between  $C_b$ , which is the bulk concentration, corresponding to the junction depth and  $C_0$  (in the most common cases  $C_b \ll C_0$ ) (Fig. 3(b)). In a similar way it was calculated [14] the average conductivity  $\sigma_m$  of the boron doped layer as  $\sigma_m = 0.39 q\mu_o C_0 + 0.59 qCo^{1/4} N_{ref}^{3/4} \Delta\mu \equiv \sigma_{om} + \sigma_{cm}$ , where  $\Delta\mu$  is the difference between the maximum and minimum value of the hole mobility on the  $C$  variation range in the empirical formula used in SUPREM process simulator [15],  $\sigma_{om}$  is a fundamental term earlier deduced [12] considering that the average conductivity would be entirely represented by a layer near the surface concentration ( $C > 5 \times 10^{19} \text{ cm}^{-3}$ ) and  $\sigma_{cm}$  represents our correction term, contributing to the full description of  $\sigma_m$  on the entire concentration range (Fig. 3(c)).

The full diffusion profile, including the variation of  $C$  in the intrinsic range ( $C < C_i = n_i$ ) was simulated taking into account that  $D = D_i$  ( $D_i$  is a temperature dependent quantity only for a certain impurity), so that the following corresponding solution of the diffusion equation, represented in Fig. 3. (a) as an extension of the extrinsic profile it was obtained [16]:

$$C = C_i \frac{\text{erfc}(x/2\sqrt{Dit})}{\text{erfc}(x_i/2\sqrt{Dit})} \quad (7)$$

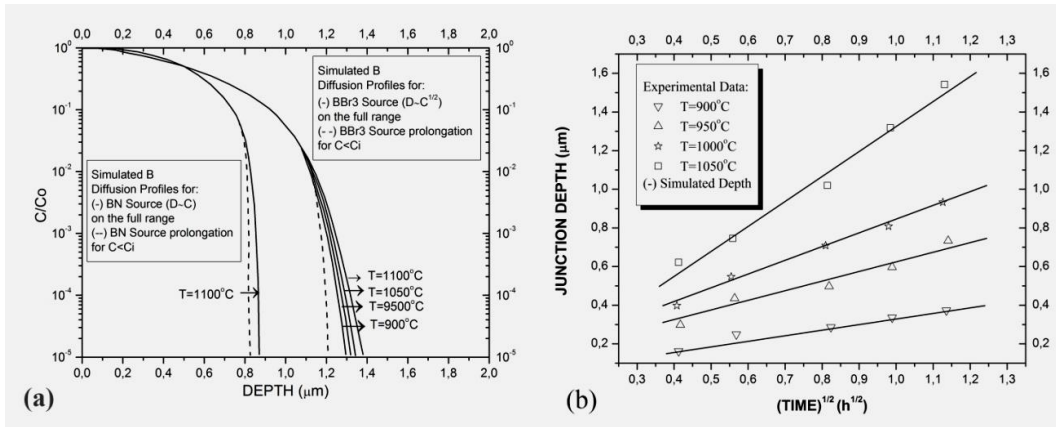


**Fig. 4.** (a) Simulated boron diffusion profile in silicon both on the extrinsic (universal curve) and intrinsic region for various diffusion temperatures after diffusion from  $\text{BBr}_3$  and for  $T=1100^\circ\text{C}$  after diffusion from BN source. (b) The corresponding junction depths described by rel. (7), well supported by the experimental data [10].

Whereas the boron diffusion from a  $\text{BBr}_3$  source system (including a reactive component (oxygen) into the furnace tube) can be accurately described considering a dependence  $D \sim C^{1/2}$ , we shown [6] that the boron diffusion from a boron nitride (BN) source (non oxidizing conditions) is suitably described by  $D \sim C$  (Fig. 5(a) and (b)) and a corresponding solution of the diffusion equation on the extrinsic range as follows:

$$x/1.6\sqrt{Dot} = 1 - 0.78(C/Co) - 0.152(C/Co)^2 \quad (8)$$

which can be extended in the intrinsic range on a similar way as in the previously discussed case, as it can be seen in Fig. 4(a).

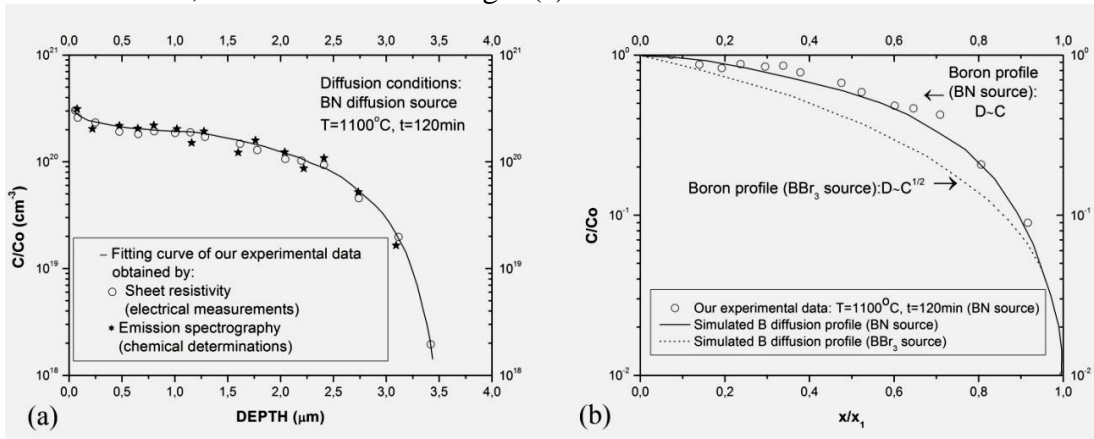


**Fig. 5.** (a) Experimental boron diffusion profile in silicon after diffusion from BN source (non oxidizing conditions). (b) Simulated profile corresponding to  $D \sim C$  (rel. (8)) compared with the profile after the diffusion from a  $\text{BBr}_3$  source.

Our reported results [6] suggests that the surface atomic processes (oxidation, as a generator of self-interstitial atoms [17]) during the boron diffusion from  $BBr_3$  source should be responsible for the modification of the profile shape observed after the diffusion from the BN source (under non oxidizing conditions), which is typical for a vacancy mechanism.

These results were taken as a reference to develop a new diffusion model including the self-interstitials as a co-participating transport current for B atoms [18] and successfully contributed to B diffusion modeling according both to Fair's concepts on the transport agent (vacancies) [8] and to Gösele's ones (self-interstitials) [17].

### 2.3. Simulation of phosphorus diffusion in silicon

Considering the previous results [19] on the three distinct regions of the phosphorus diffusion profile,  $D \sim C^2$  on the flat region near the surface, delimited by the electrically active phosphorus concentration ( $n_s, n_1$ ), then  $D \sim C^{-2}$  on the next transition region delimited by the concentration range ( $n_1, n_2$ ) and  $D = Di$  in the bulk (intrinsic) region after the diffusion by thermo – chemical technique ( $POCl_3$  source), an analytical solution on each range of three coupled nonlinear diffusion equations we found both for shallow [20] and deeper junctions [21] (for instance corresponding to diffusion temperature of  $1100^\circ C$ ), able to accurately describe the phosphorus profile, as it is shown in Fig. 6 (a) and (b), as follows:

$$N_1 = n_s \{ [1 - (1 - n_1^3)X/2X_{e1}]^{1/3} \} \quad (9a)$$

$$N_2 = n_{e1}(X_{e2} - X_{e1}) / [(X_{e2} - n_2X_{e1}) + (n_2 - 1)X] \quad (9b)$$

$$N_3 = n_{e2} \operatorname{erfc} X / \operatorname{erfc} X_{e2} \quad (9c)$$

where

$X_{e1} = x_{e1}/2 (\sqrt{D_3 t})$ ,  $X_{e2} = x_{e2}/2 (\sqrt{D_3 t})$ ,  $X = x/2 (\sqrt{D_3 t})$ ,  $n_1 = n_{e1}/n_s$ ,  $n_2 = n_{e1}/n_{e2}$ , and the concentration of the electrically inactive phosphorus atoms is given by the empirical relation [19]:

$$C = n + 2.04 \times 10^{-41} n^3 \quad (10)$$

The value of the concentration  $n_{e2}$  has to be computed from the implicit relation:

$$X_{e1} \exp(-X_{e1}^2) / \operatorname{erfc} X_{e1} = (\sqrt{\pi} / 6) \{ (n_{e2}/n_{e1}) [(n_s/n_{e1})^3 - 4] + 3 \} \quad (11)$$

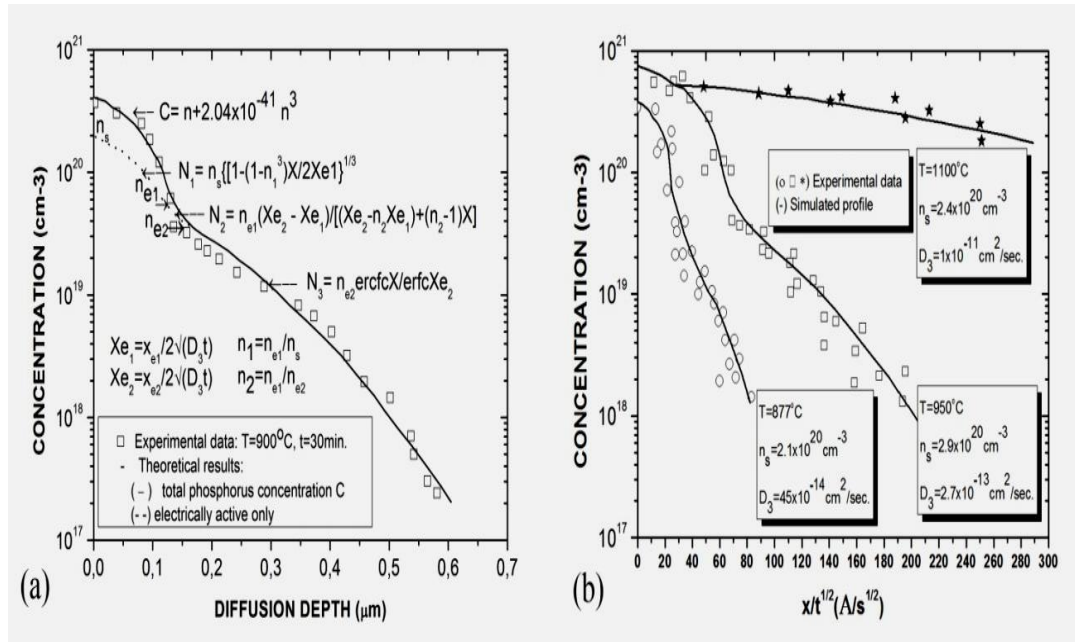


**Fig. 6.** (a) Simulated phosphorus profile on the three regions (our results [20,21]), defined by the corresponding depths  $x_{e1}$  and  $x_{e2}$ ,  $n_s = N_I(x=0)$ ,  $n_{e1} = N_I(x_{e1})$ ,  $n_{e2} = N_2(x_{e2})$ ,  $N$  being the active phosphorus concentration, compared with experimental data [21]. (b) Simulated phosphorus profiles for various temperatures, compared with experimental data [19].

The very good agreement of our theoretical results with the experimental data on the usual concentration range well support the simulation analytical relations, which become a versatile and rapid set of expressions to describe accurately the phosphorus diffusion profile.

#### 2.4. Simulation of antimony diffusion in silicon

Although it has been believed that Sb diffusion in silicon has been occurred by a vacancy mechanism, there were not clear evidences reported in the literature to demonstrate this situation.

Analyzing the Sb diffusion profile after the diffusion in 100% Ar (not oxidizing atmosphere) at the temperature of 1250 C for 4 hours reported in [22], we demonstrated that the Sb diffusion coefficient depends on the concentration as  $D \sim C$ , as it can be seen in Fig. 7 (a) and then it is possible to describe accurately this profile in extrinsic range of the concentration by an equation of the form (8) [23].

Moreover, comparing the experimental data with our theoretical results on the intrinsic range, described by an equation form of (7), the agreement between these data is very good, well supporting our theoretical model [24].

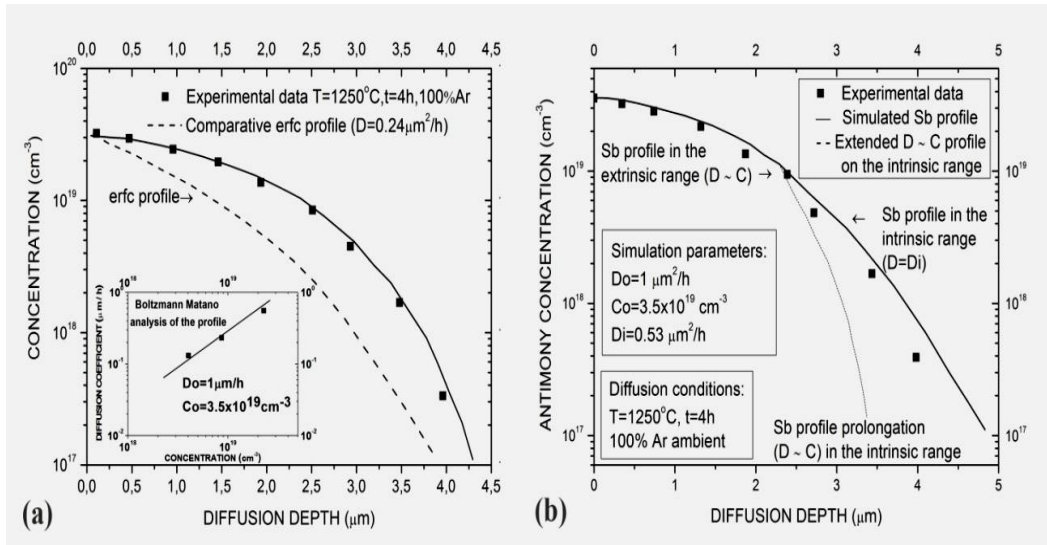


**Fig. 7.** (a) Experimental Sb profile after diffusion at  $T=1250^{\circ}\text{C}$  for 4 hours in 10% Ar [22] compared with classical (erfc type profile); inside of this graph are inserted the results of Boltzmann-Matano analysis of the experimental profile, demonstrating that  $D\sim C$ . (b) The simulated Sb diffusion profile both in the extrinsic and intrinsic range according to our theoretical relations [23, 24].

We demonstrated in this way that Sb diffusion profile after the conventional diffusion shows a dependence  $D\sim C$ , which is characteristic for a vacancy diffusion mechanism and can be accurately described both in the extrinsic and intrinsic range of the concentration.

### 2.5. Assessment of the impurity redistribution after the oxidation process

In Fig. 8(a) there are presented our experimental results on the redistribution profiles after boron diffusion at  $T = 950^{\circ}\text{C}$  for a time period of 15 min from a BN source and a second oxidation step at  $T = 1150^{\circ}\text{C}$  for 10 min in oxygen atmosphere and 10 min in neutral nitrogen flowing gas.

In the same figure is shown the phosphorus profile after the doping (diffusion) step at  $800^{\circ}\text{C}$  for 10 min from  $\text{POCl}_3$  source and the oxidation at  $1200^{\circ}\text{C}$  for 10 min in oxygen and 10 min in nitrogen flowing gas, compared with the classical Gauss profile.

These profiles were obtained by the successive removal of thin silicon doped layers and the measurement of the sheet resistivity, as it was described for the determination of the high concentration phosphorus diffusion profile described earlier [4].

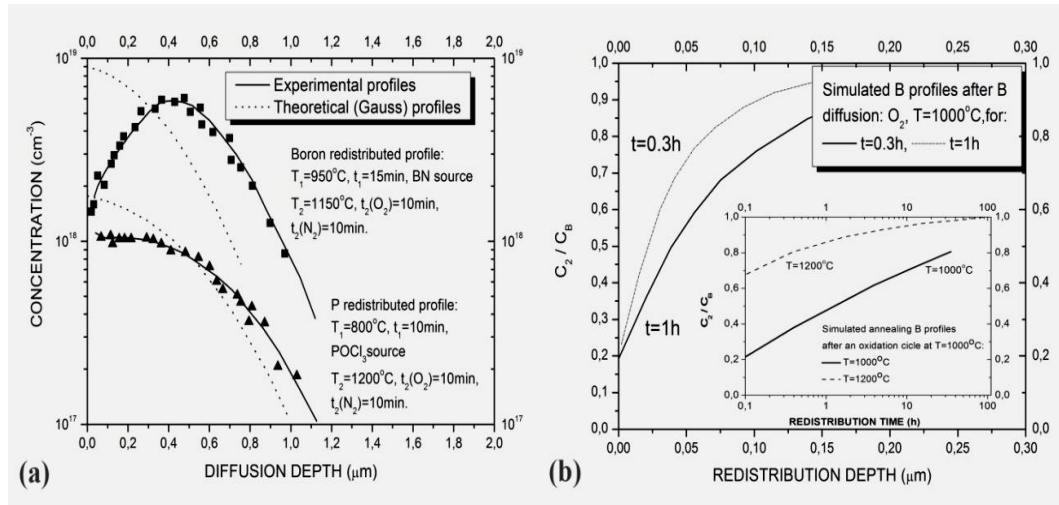


**Fig. 8.** (a) Experimentally determined boron and phosphorus diffusion profile after a first doping (diffusion) step and redistribution during a second step in oxygen and nitrogen ambient as indicated in the inserted data. (b) Simulated boron concentration profiles ( $C_2$ ) near the silicon/SiO<sub>2</sub> interface after oxidation cycles at  $T=1000^\circ\text{C}$  for 0.3 h and 1h with respect to the bulk uniform value ( $C_B$ ) and the recovery of  $C_2$  during the redistribution step in a nitrogen ambient [25] (inserted graph).

As it can be seen in Fig. 8(a), the boron diffusion profile after the two steps of diffusion shows an important deviation from the Gauss type profile near the surface, consisting in a decrease of the boron concentration on an extended region with respect to the bulk Gaussian profile, as a consequence of the oxidation process. As the fabrication of the field effect transistors is sensitive to the concentration profile in this zone, it is of real importance the control the redistribution profile in this region, the interest being in a uniform distribution of the concentration. This problem was solved as a solution of the diffusion equation [25] and it was assessed the recovery redistribution profile as it is shown in Fig. 8(b), where it can be seen that the initial uniformly distributed boron concentration is modified by a concentration decreasing near the silicon/SiO<sub>2</sub> interface after the oxidation processes and the recovery is quite slow at low temperatures (smaller than  $1000^\circ\text{C}$ ) and becomes significant at temperatures of the order of  $1200^\circ\text{C}$  after the boron redistribution in neutral nitrogen ambient (inserted graph in Fig. 8(b)).

### 3. Simulation of the impurity diffusion from implanted layers

The diffusion from the implanted layers is one of the most advantageous alternatives to the thermo-chemical doping taking into account the better control of the amount of the impurities and the uniformity and reproductivity of the process. However, the implantation process is associated with an obligatory annealing step necessary not only to redistribute the implanted impurity to obtain a desired junction depth but also to anneal satisfactorily the damages produced by the implantation process.

We approached the description of the diffusion profile after post-implantation thermal annealing and after laser-assisted annealing, as it will be shown as follows.

### 3.1.1. Simulation of the post-implantation antimony diffusion profile

In Fig. 9 (a) it is shown the Sb simulated profile after an implantation at low dose ( $N = 10^{14} \text{ cm}^{-2}$ ) and energy ( $E = 20 \text{ keV}$ ) assuming that there were not impurity losses during the post annealing process at the temperature  $T = 900^\circ\text{C}$  for various annealing time. The agreement between the simulation and the experimental data shown in Fig. 9 (b) well supports the proposed theoretical model, allowing the extraction of the constant value of the diffusion coefficient during the post-implantation process [26].

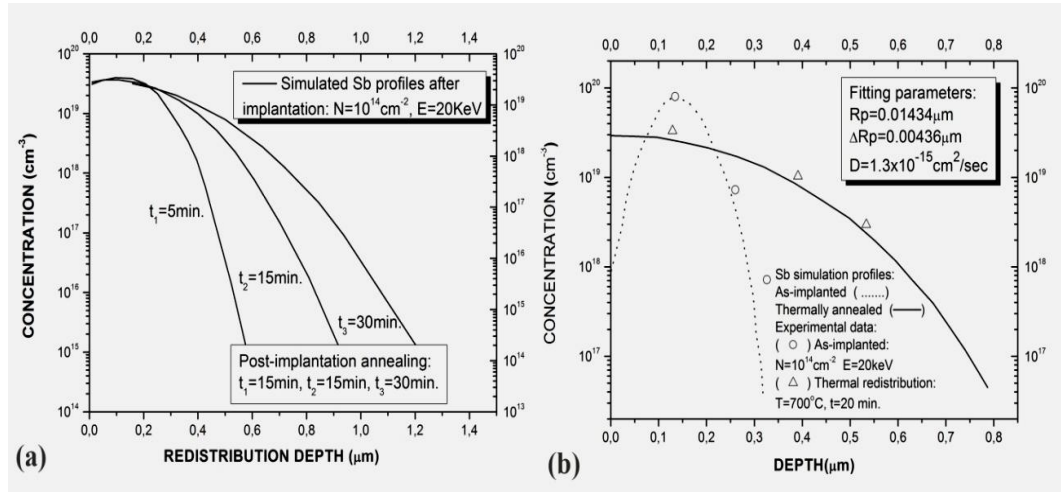


**Fig. 9.** (a) Simulation of Sb annealing process for 5 min, 15 min and 30 min at  $T=700^\circ\text{C}$  after an implantation process with a dose  $N = 19^{14} \text{ cm}^{-2}$  and an energy  $E = 20 \text{ keV}$ .

(b) Comparison of the simulated Sb profile after a post-implantation annealing at  $T = 700^\circ\text{C}$  for 20 min with the experimental data [26], under the conditions of the implantation data of Fig. 9 (a);  $R_p$  is the projected range and  $\Delta R_p$  is standard deviation of the profile after the implantation.

### 3.1.2. Simulation of the diffusion from the buried and surface implantation local sources

The specific profile after the implantation, showing a maximum of the doping concentration in the silicon bulk and a rapid decreasing concentration near the silicon surface depending on the implantation energy is favorable to avoid the self-doping of the silicon substrate before the epitaxial growth process in the integrated circuit manufacturing for the realization of the isolation walls by a buried and/or surface doping source [27-30] and we simulated it under various conditions [31-33] in order to describe a large range of useful applications as

multisequential annealing, with and without impurity losses, laser – assisted annealing, surface and buried source redistribution process, redistribution with fixed boundary or during a moving boundary process like the epitaxial growth.

In Fig. 10 (a) it is shown a schematic representation of a silicon microstructure isolation realized by the boron diffusion from a buried and a surface implanted source allowing the concomitant epitaxial growth and the boron diffusion during the thermal process and the substantial reduction on this way of the fabrication time. However, in order to optimize this process (to avoid concomitantly the lateral self-doping of the silicon layer with boron atoms from the local implanted source and the loss of a significant quantity from this source during the pre-epitaxial etching process), it was necessary to dispose of a solution of the diffusion equation to describe the post-implantation redistribution during the multi-sequential thermal processes, taking into account also the possible ex-diffusion and the displacement of the silicon surface due to the etching pre-epitaxial process (moving boundary), as it was presented in [31-33]. A simulation example to obtain the optimal process conditions with respect to the implantation energy  $E$ , the implantation dose  $N$ , the etching process with the rate  $\nu$ , on the base of our analytical results is shown in Fig. 10 (b), considering the etching pre-epitaxial time  $t$  as a parameter.

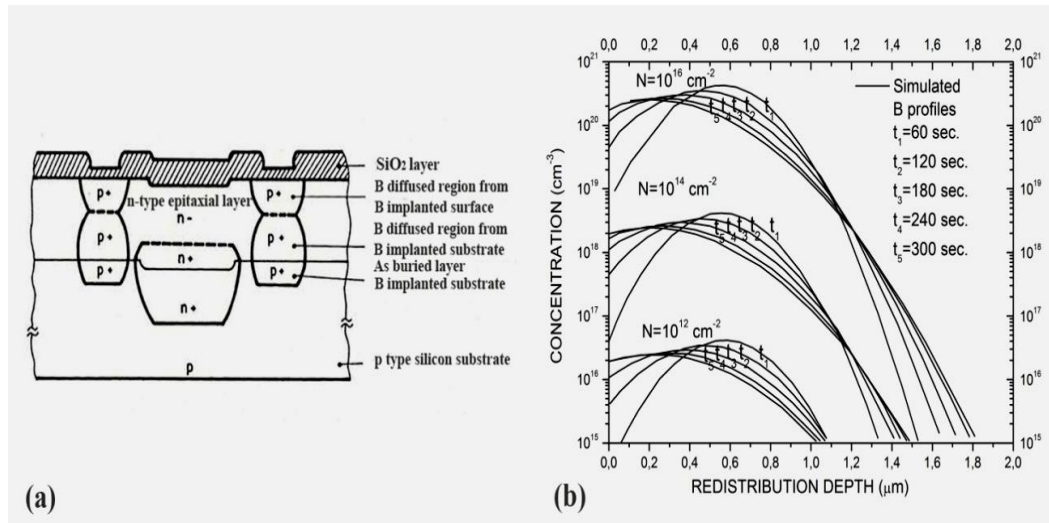


**Fig. 10.** (a) Schematic representation of a silicon microstructure cross section isolated by the surface and buried local implantation source.

(b) Simulated boron diffusion profiles as a function of the optimizing process parameters: dose  $N$  and pre-epitaxial etching time  $t$  after a boron ion implantation with the energy  $E=300$  keV [33].

### 3.1.3. Simulation of the laser-assisted redistribution after the impurity implantation in silicon

As an alternative technique for the recovery after the impurity implantation in silicon, the laser-assisted annealing presents the advantage of shorter process [34]. However, the use of pulsed-laser for the post-implantation annealing of semiconductors (particularly of dopant impurity implanted in silicon) requires the knowledge of the laser-induced thermal regime, i.e. the spatial and temporal evolution of the laser-induced temperature in the irradiated solids, with respect of the material characteristic parameters. We deduced the induced temperature as a solution of the heat transport equation in solid under certain conditions, as presented in Fig. 11 (a), describing the distribution of the temperature in solid as a function of the heat diffusion length both in the turn-on and turn-off stage for a pulse duration  $\tau=10^{-4}$  sec and the process time  $t$  as a parameter in the case on the silicon is not melted.

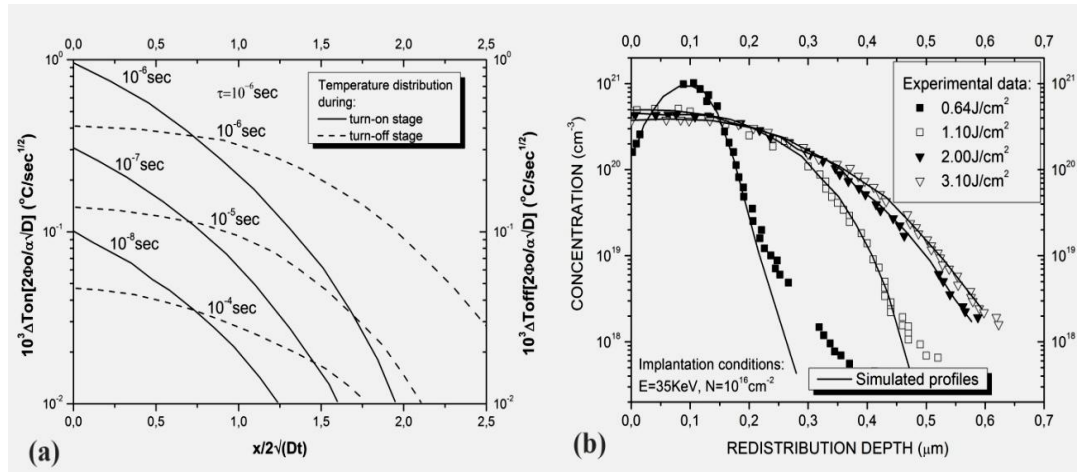


**Fig. 11.** (a) Simulated temperature depth distribution in silicon [35] during a pulsed ruby laser turn-on stage (left vertical axis) and a turn-off stage (right vertical axis) with time as a parameter during and after a pulse of  $10^{-4}$  sec. (b) Simulated boron diffusion profiles after various values of the energy density of a ruby pulse laser [36].

In Fig. 11. (a)  $D$  is the heat diffusion coefficient,  $\alpha$  the absorption coefficient of the radiation,  $\Delta T$  is the temperature variation with respect to the ambient one and  $\Phi_0$  is the absorption irradiation flow depending on the energy density of the laser and on the material parameters [35].

A substantial redistribution of the main doping impurities (B, P, As) in silicon has been observed after the post-implantation annealing process performed by using a ruby pulsed laser for short time (of the order of  $10^{-7}$ - $10^{-8}$  sec.) [34], which can be explained by the impurity diffusion during a melt-phase of the implanted silicon layer [36].

We succeeded to describe analytically the impurity redistribution after ionic implantation and laser post implantation annealing (pulsed laser melting and recrystallization process) [36] by surpassing of the theoretical complications coming from the time dependence of the pulsed laser temperature and corroborating with our approached form for the impurity post implantation redistribution [32], so that a very good agreement with the experimental data represented in Fig. 11 (b) and 12 (a) it was obtained.

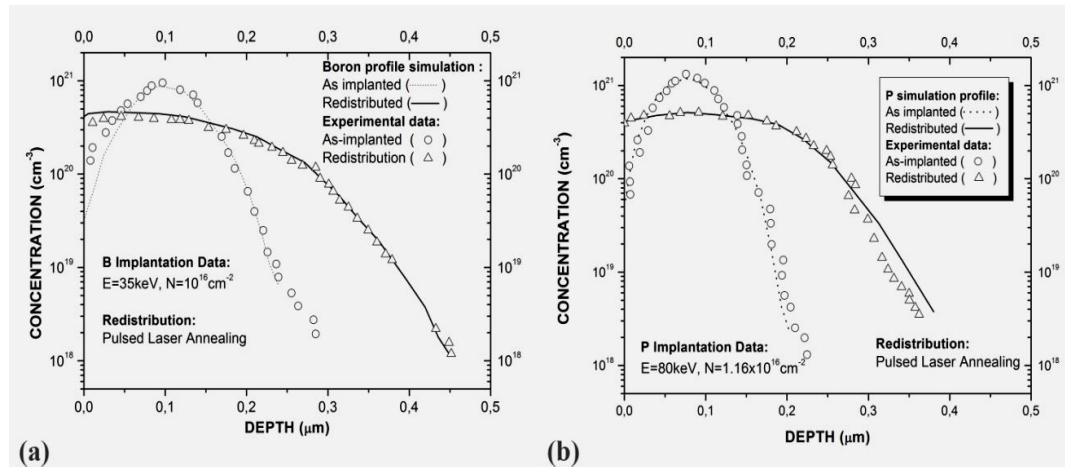


**Fig. 12.** Simulated redistribution profile in [100] oriented silicon [36] after a pulsed ruby laser annealing (radiation length  $\lambda=0.69\mu\text{m}$ ) with a density of energy in the range  $1.5\text{-}1.7\text{ J/cm}^2$  corresponding to: (a) boron implanted impurities; (b) phosphorus implanted impurities.

Similar results we obtained to simulate the phosphorus, arsenic and antimony redistribution after a ruby pulse laser annealing, as it is shown in Fig. 12 (b) and Fig. 13 (a) and (b) respectively.

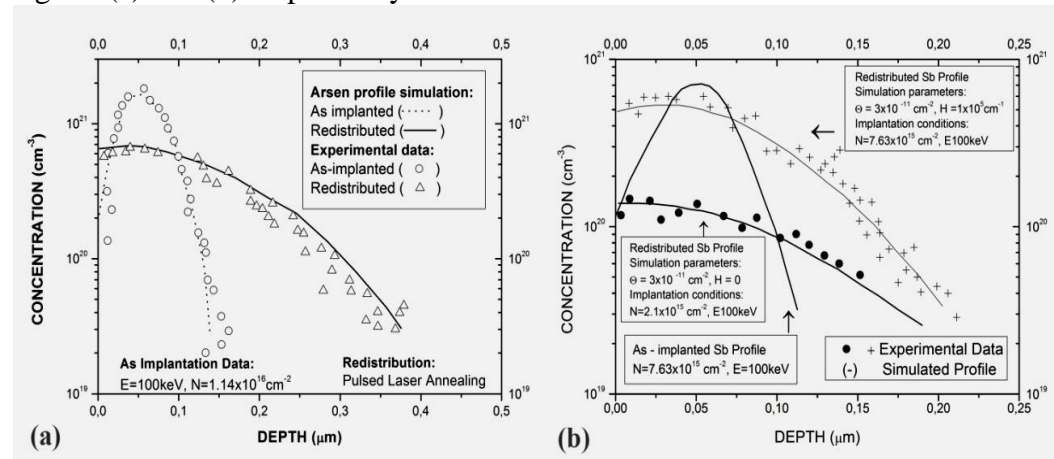


**Fig. 13 (a).** Simulated arsenic redistribution profile silicon after a pulsed ruby laser annealing [36].  
**(b)** Simulated antimony redistribution profile with and without surface impurity losses [37, 38].

The profiles of Sb after the post implantation laser annealing with and without impurity losses through the external silicon surface were also well described by suitable analytical approximations, as it is shown in Fig. 13 (b) [37, 38]. In this case a suitable solution of the diffusion equation was necessary to be deduced including in an explicit form the Sb out-diffusion from the silicon surface during the annealing process in order to correctly describe the redistribution profile (Fig. 13 (b)), by including a parameter  $H$  of the out-diffusion in the surface diffusion conditions and a redistribution length  $\theta$  which includes, besides the standard deviation  $\Delta Rp$  of the implanted profile, an integrated redistribution coming from the time-dependent diffusion coefficient, so that a close approximation useful for the full description of the laser-assisted post-implantation process was successfully obtained [36-38]. The very good agreement of our theoretical considerations and results with the experimental data, well support our modeling and simulation, by a successful ability to describe in this way the phenomena intervening in such a complex redistribution process (pulsed laser melting and re-crystallization process, time-dependent diffusion coefficient of the heat transmission in silicon). Successful results were obtained also on a modelling of heat transmission in multilayer solids with cylindrical symmetry in a microstructure power heating system for industrial application [39].

### 3.2. Simulation of the impurity profile after the diffusion from polysilicon layers

Extending our researches to the diffusion from polysilicon sources, we had shown that a suitable analytical description of the boron and arsenic diffusion profile in silicon [40] is obtained taking into account rel. (3) and (8) respectively, the diffusion coefficient of the arsenic exhibiting a concentration dependence on the form  $D \sim C$ . The comparison between our theoretical results and the experimental data [41] well supports our models (Fig. 1). Our results constitute therefore a valuable alternative to the complicated numerical computation software models included in SUPREM and ICECREM simulators [42].

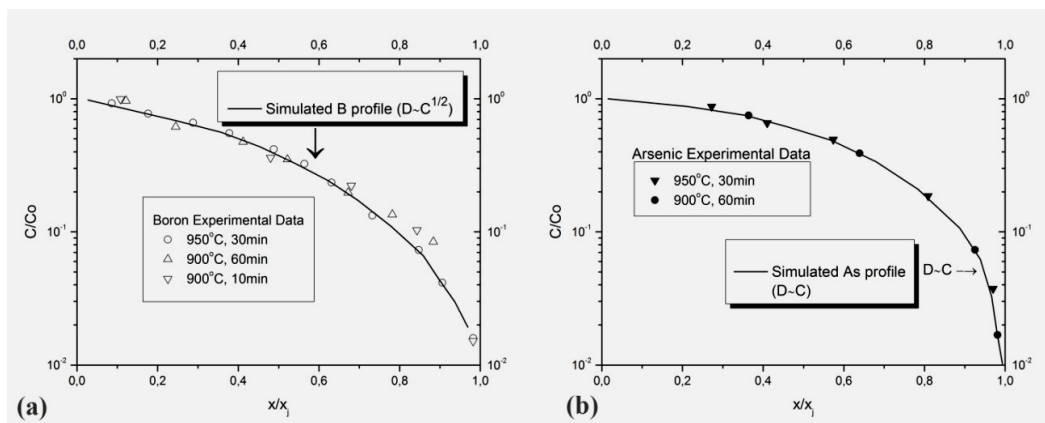


**Fig. 14.** (a) Boron and (b) arsenic simulated diffusion profiles in silicon after diffusion from polysilicon doped source [40] compared with experimental data [41].

Due to the low defect density induced in the processed bulk, the implanted polysilicon layers sources are useful for the fabrication of the integrated circuits with shallow junctions and are suitable for the microfabrication of high efficiency bipolar transistors and MOS type devices [42].

### 3.3 Simulation of the impurity diffusion in multilayers systems

Versatile analytical results able to describe the impurity diffusion from [43, 44] and through [45] a multilayer system on silicon (and on GaAs for Zn diffusion), as non-conventional diffusion techniques with applications in the shallow junction technology were also obtained, useful both for further theoretical developments (simulation of diffusion in regions with  $D=D(x)$ , for instance near the Dielectric/Si interfaces) and for the simulation of the diffusion from a  $\text{SiO}_2/\text{Doped-SiO}_2$  source in silicon.

In Fig. 15 (a) is shown an example of the simulation of the impurity diffusion from an infinite source (not consumable during the diffusion process) into a system of three components, the last one being a semi-infinite semiconductor [43]. The variation with the depth of the impurity concentration in each of the system component results as an infinite series of erfc-type functions, but in the practical cases only a few first terms contribute significantly (depending on the desired accuracy) to describe the impurity diffusion profile (Fig. 15 (a)), even the first term only Fig. 15 (b)).

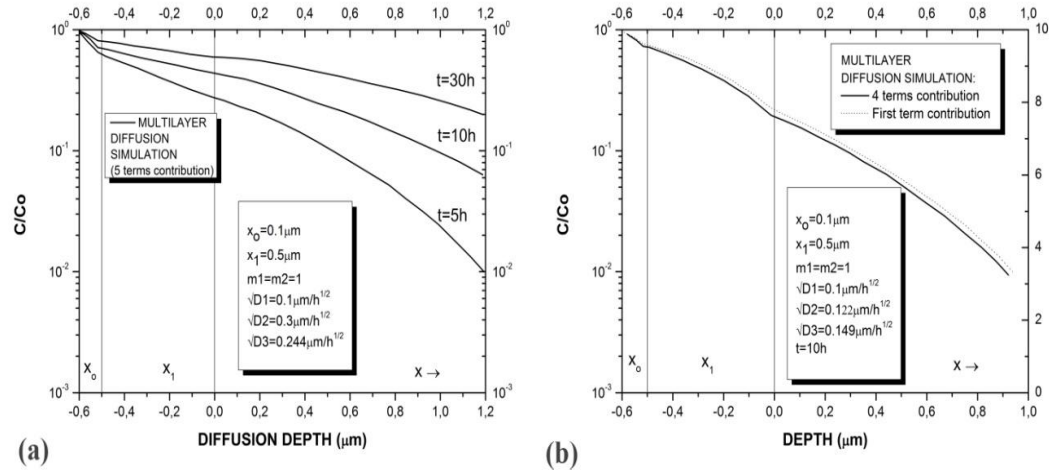


**Fig. 15.** Simulation of the impurity diffusion in a system with three components including 5 terms of the convergent series (a) and only the first one (dashed line), compared with a calculated profile including 4 term contribution (solid line) [43] (b), showing a rapid convergence of the series.

An interesting situation is the diffusion in a multilayer system consisting in an external local deposited source deposited onto the semiconductor surface, which can be protected or not [44, 45], the protection consisting in an external layer (for instance  $\text{SiO}_2$ ).

The protected source can be a  $\text{SiO}_2$ /(Doped  $\text{SiO}_2$ )/(External Protection  $\text{SiO}_2$ ) system deposited during the same technological process into the same tube on the silicon or GaAs wafer (or other type of semiconductor compounds), the protection referring to the oxide barrier properties against the impurity out diffusion from the local doped source layer during the thermal processing [46, 47].

As the impurity still can escape from the local source (Doped  $\text{SiO}_2$  layer) to the external ambient through the protection  $\text{SiO}_2$  layer, depending on the diffusion length with respect to the thickness of the protection layer, this would be a Partially Protected (PP) source, in opposition with the Entirely Protected (EP) source [45]. Solutions of the diffusion equations were given for Unprotected Sources (UP), EP and PP systems and simplified forms suitable for rapid evaluations were deduced in that cases [45].

Such sources are widely used for the fabrication of thick doped layers of the high power transistors and/or for isolation wall of the integrated circuits.

Special applications are also noticeable for low doped layers and for the fabrication of GaAs luminescence diodes [46, 47].

In Fig. 16 (a) is demonstrated that  $D = \text{const}$  ( $D$  does not depend on concentration) on the intrinsic range considered in our modelling [45] is a realistic assumption and in Fig. 16 (b) the possibility to obtain very close performances by using PP sources (easier to be obtained during a continuous process in the tube, as discussed above) instead of an EP source (ideal from the protection point of view).

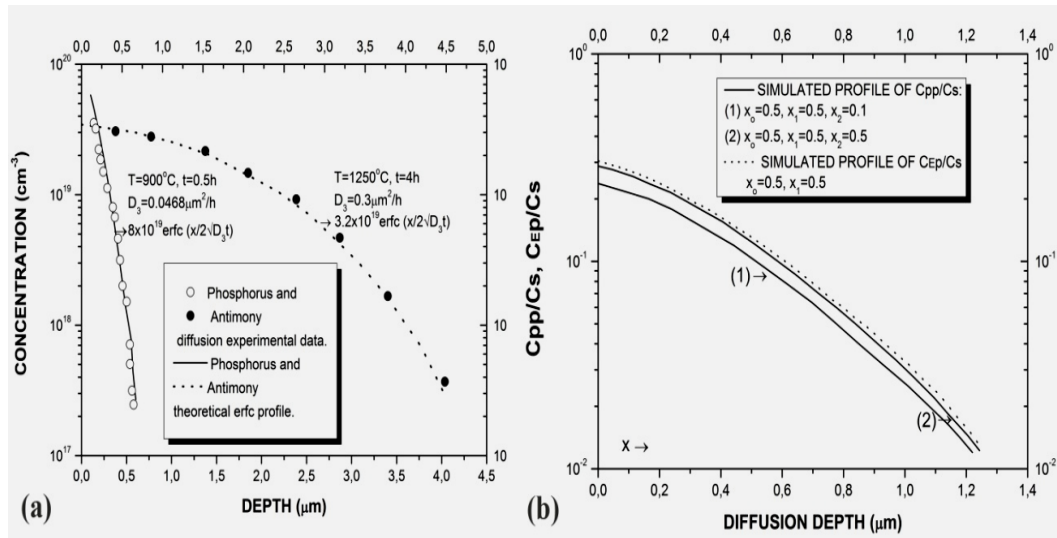


**Fig. 16.** (a) Simulated diffusion profiles of phosphorus and antimony in silicon on the intrinsic range by using the typical erfc function, denoting that  $D=\text{const}$ . (b) Comparison between the close performances of a partially protected (PP) source and of an entirely protected (EP) source represented as normalized concentration ( $C_{pp}/C_s$ ,  $C_{ep}/C_s$  where  $C_s$  is the surface value) vs. the diffusion depth.

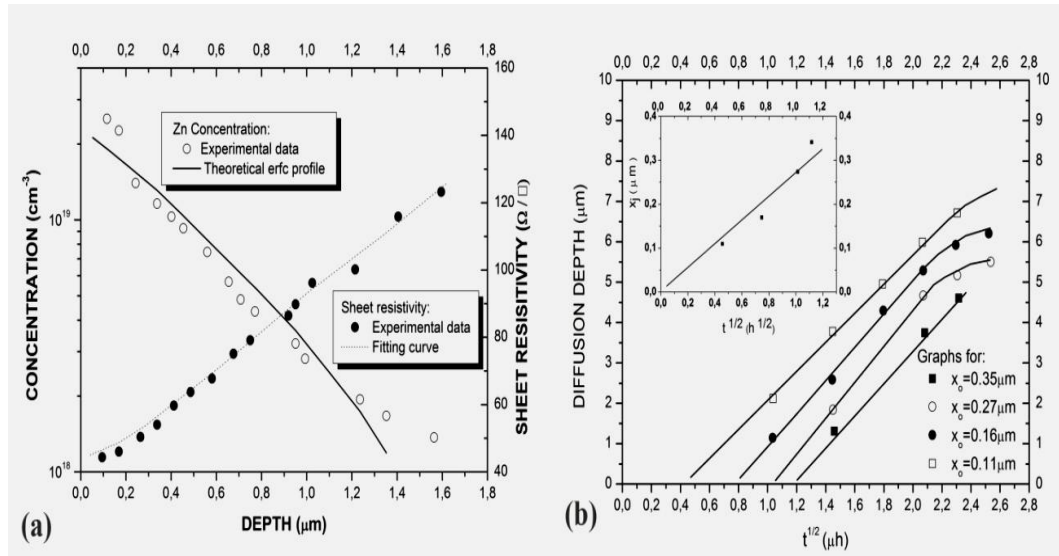


**Fig. 17.** Our experimental results on Zn diffusion in GaAs through a SiO<sub>2</sub> layer:  
 (a) Zn profile fitted by an erfc type theoretical profile ( $D=\text{const.}$ );  
 (b) Zn depth dependence on the square root of the diffusion time in GaAs and in SiO<sub>2</sub> layer (inserted graph).

In Fig. 17 (a) is shown the variation of the Zn concentration with the depth in GaAs which we obtained by successive removals of thin doped GaAs layers and sheet resistivity measurements after Zn diffusion from a local doped source through a SiO<sub>2</sub> layers in the GaAs wafer, demonstrating that this profile follows an erfc type variation ( $D = \text{const}$ ) [45].

In Fig. 17 (b) are presented our experimental results on Zn diffusion in the same system, showing a dependence of the junction depth on the square root of the diffusion time [47], which is characteristic for the assumed model [45].

By a suitable extrapolation procedure there were obtained similar results showing the behaviour of Zn diffusion in the SiO<sub>2</sub> layer (inserted graph in Fig. 17 (b)) [47].

#### 4. Misfit stress and misfit dislocations induced by the impurity diffusion in silicon

Due to the mismatch between the radius of the impurities diffusing in silicon and that of the host atoms, an elastic stress is induced in the silicon wafers, which can generate under some critical conditions a dense area of misfit dislocations, affecting the quality of the electrical junction properties like the reverse current through a  $p-n$  junction, the breakdown voltage [48], the recombination current [49], specifically observed after the fabrication of the  $pnp$ -type switching transistors and integrated circuits due to the precipitation of the electrically active metallic impurities like gold [50] and not only.

#### 4.1 Evaluation of the misfit elastic stress induced by the impurity diffusion in silicon

Focusing our investigations on the critical conditions for the generation of the misfit dislocations in silicon induced by the impurity diffusion in silicon, we dedicated an especial attention to the suitable techniques to reveal the dislocations [51] both on the fabricated microstructure of the integrated circuits after the boron diffusion and on the processed silicon wafers (Fig. 18 (a)), and on the evaluation of the misfit elastic stress induced by the diffusion in silicon, specifically after the boron implantation and post-implantation annealing [52, 53] (Fig. 18 (b)).

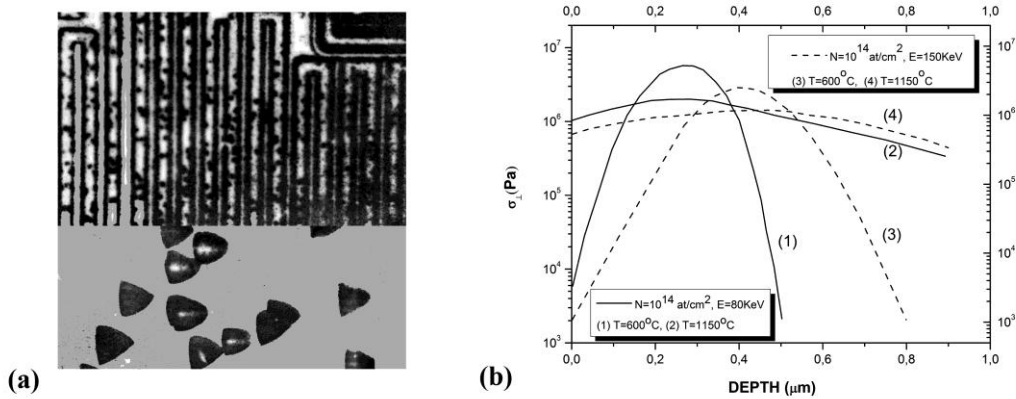


**Fig. 18.** (a) Boron diffusion induced dislocations revealed by preferential etching technique on an integrated circuit microstructure (superior side) and on the silicon wafer (inferior side of the figure) [51]. (b) Simulation of the misfit elastic stress induced by boron implantation with a dose  $N = 10^{14} \text{ cm}^{-2}$  and with the energy  $E = 80 \text{ keV}$  (full line) and  $E = 150 \text{ keV}$  (dashed line) and post-implantation annealing at the temperatures  $T = 600^\circ \text{C}$  and  $T = 1150^\circ \text{C}$  for a time  $t = 30 \text{ min}$  in typical silicon wafers of  $250 \mu\text{m}$  thickness used for microstructure fabrication [52, 53].

Calculating the elastic stress induced by the boron implantation in silicon, we shown [52] that the variation of the stress perpendicular on the diffusion direction  $\sigma_{\perp}$  in a silicon wafer of the thickness  $2a$  follows mainly the doping profile variation (Fig. 18 (b)), the terms expressed as a function of  $(L/a)$  and  $(L/a)^2$ , where  $L$  is the effective diffusion length, representing corrections of the first and second order respectively [52] because in the most applicable cases  $L/a \ll 1$ . These results allow calculating the elastic stress induced in the silicon wafers by ion implantation and subsequent annealing at a function of the process conditions: implantation dose, implantation energy and the diffusion time and temperature. On this basis we explained the drastic reduction with two orders of magnitude of the density of the boron implantation dislocations loops after a second step of annealing, [53] by the contribution of the driving force induced by the mismatch stress to the dislocation climbing or gliding process to the silicon surface, where these dislocations are annihilated by a relaxation mechanism.

## 4.2 Critical conditions for the generation of misfit dislocations induced by boron diffusion in silicon

Due to the mismatch between the impurity and the silicon lattice atom radius at high boron concentration, a dense misfit array of boron induced dislocations is generated within a region near the surface limited in the silicon bulk by the plane of maximum gradient [54], and based on that our assumption, we calculated the critical conditions of the generation of misfit dislocations by means of rel. (3) and we expressed these conditions in terms of variation  $C_0$  vs. diffusion depth (Fig. 18 (a)),  $C_0$  vs. the critical diffusion time (Fig. 19 (a)) and critical time vs. temperature (Fig. 19 (b)), and we analysed by secondary ion mass spectroscopy (SIMS) and the bevelled angle selective chemical etching (BASCE) advanced techniques the boron induced misfit dislocations after diffusion from BN source [55] with further applications on the control of the boron induced stress in thin silicon membranes obtained by bulk micromachining technology [56].

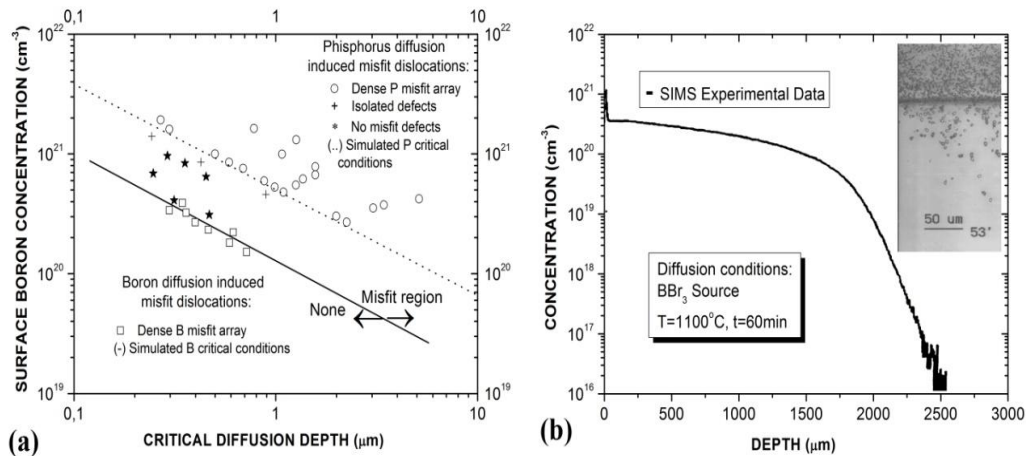


**Fig. 18.** (a) Surface boron concentration as a function of the critical diffusion depth according to our model [54] (full line) compared with our experimental determinations [55] and with the phosphorus critical conditions (dashed line) [59]. (b). SIMS determined boron diffusion profile after a diffusion from  $BBr_3$  source at  $T=1100^\circ\text{C}$ ,  $t=60\text{min}$  and the BASCE corresponding misfit dislocations (inserted photo) determined under an angle of  $53^\circ$ .

In Fig. 18 (b) is shown a typical boron profile after 1 hour diffusion from  $BBr_3$  source at  $1100^\circ\text{C}$  determined by SIMS technique and the corresponding misfit dislocation area (inserted photo) revealed by BASCE technique [55], allowing the extraction of the useful data to compare our theoretical model with the experimental evidence, as shown in Fig. 18 (a) for various conditions of diffusion time and temperature.

The agreement between the experimental and theoretical results well support our model.

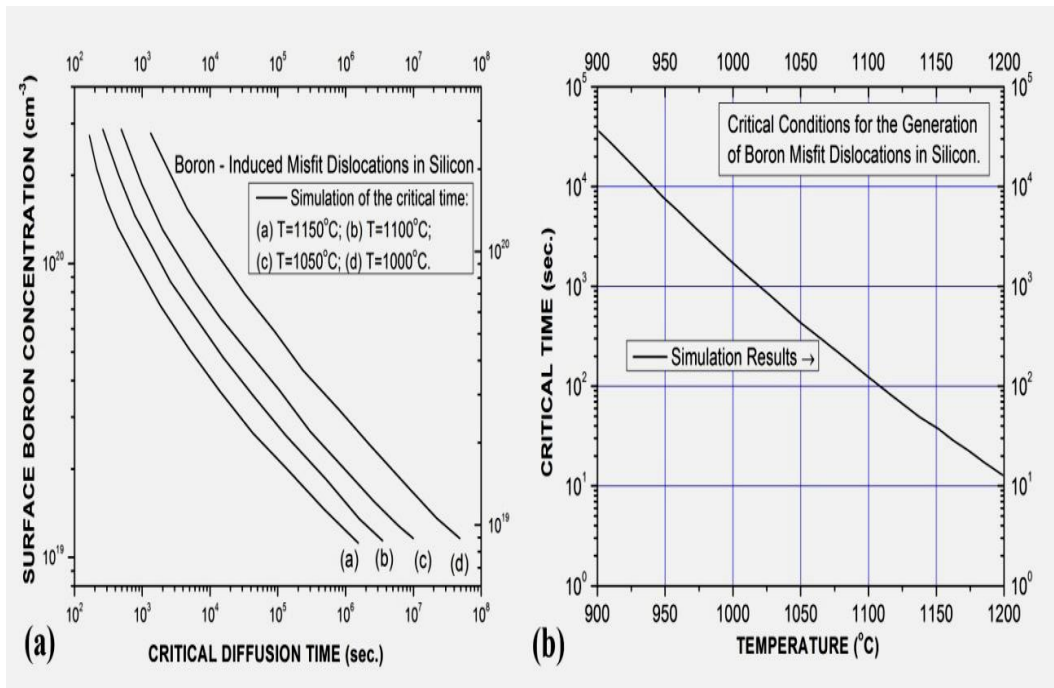


**Fig. 19.** (a) Surface boron concentration as a function of the critical diffusion time [54].  
(b) Calculated critical diffusion time as a function of the diffusion temperature necessary for the generation of the boron misfit dislocations in silicon.

In order to optimize the boron diffusion process by the minimization of the misfit stress induced in the silicon membranes for the micromachining fabrication by bulk technique of the silicon capacitive pressure sensors for biomedical applications [56], we performed some adequate experiments consisting in boron pre-diffusion from BN source (a first diffusion step) and an oxidation at high temperature in oxygen gas, applying then SIMS and BASCE determinations to observe the correlation between the diffusion conditions and the misfit dislocations.

The long-time diffusion (60 min) at high temperature (1150°C) was necessary to define sufficiently thick micromechanical elements after the chemical etching in alkaline solutions performed by the bulk micromachining technology.

A typical result is shown in Fig. 20 (a), representing the depth distribution of the dislocation density and the corresponding BASCE revealed dislocations in the inserted photo.

As it can be seen from this graph, the extended density distribution in the entire doped region after the diffusion is converted in a localized distribution with a maximum value near the maximum gradient of concentration, explained as a result of the annealing process associated with the relaxation of the induced stress.

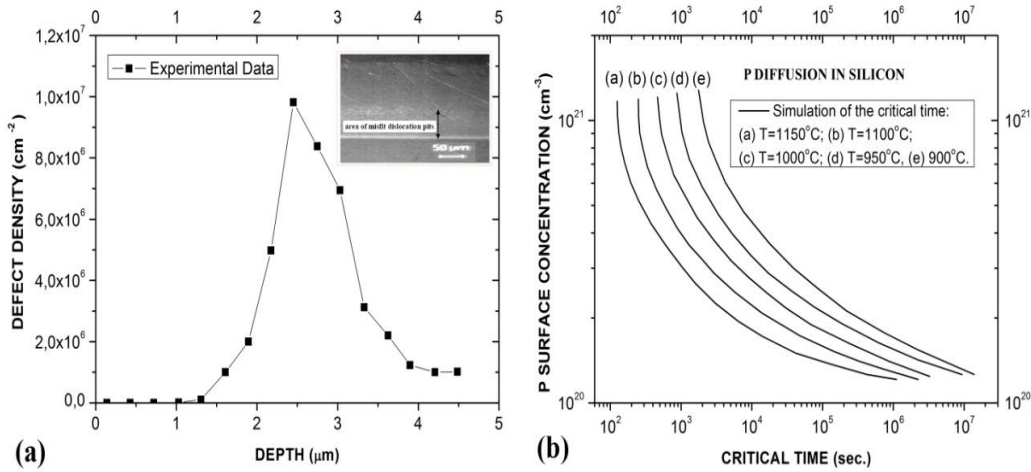


**Fig. 20.** (a) The distribution with the depth of the density of misfit dislocations after the boron diffusion performed in two steps:  $T_1 = 900^\circ\text{C}$ ,  $t_1 = 45$  min,  $T_2 = 1150^\circ\text{C}$ ,  $t_2 = 60$  min and the corresponding BASCE aria of misfit dislocations (inserted photo). (b) Simulation curves describing the critical conditions of the misfit dislocations generated by the phosphorus diffusion in silicon in terms of phosphorus surface concentration vs. critical diffusion time for various diffusion temperatures [57].

#### 4.2 Critical conditions for the generation of misfit dislocations induced by phosphorus diffusion in silicon

We calculated also in an analytical way the critical conditions for the generation of the misfit dislocations induced by the phosphorus diffusion in silicon at high concentration [57, 58], taking into account the results of our analytical model describing the phosphorus diffusion profile in silicon (rel. (9a)) and a previous model on the misfit dislocations showing that these dislocations are generated in the high concentration region near the silicon surface [59] (where the phosphorus diffusion coefficient depends on second power of the doping concentration) and the critical conditions are shown in Fig. 18 (a), compared with the corresponding experimental data [59]. Our model allowed to calculate therefore the critical conditions for the generation of the misfit dislocations during the phosphorus diffusion in silicon in terms of phosphorus surface concentration as a function of the critical diffusion time for various diffusion temperatures [57, 58] (Fig. 20 (b)) and on this way a allowing a very close control for the fabrication of high quality (low density of diffusion pipes) in *npn* transistors and integrated circuits.

#### 5. Simulation of gold diffusion in silicon and gettering phenomena

Gold is an impurity acting as a recombination centre in both p and n-type silicon and is intentionally introduced in silicon wafers by a diffusion process for the fabrication of the fast switching transistors with computer applications.

The gold diffusion in silicon can be described by a dependence  $D \sim C^2$  and by a corresponding diffusion profile shown in Fig 21(a), so that this non uniform profile modifies the ideal forward current density  $J_i$  through a p-n junction, converting it in a current density  $J$  dependent on the junction depth  $x_j$  and on the gold diffusion conditions (time and temperature) [60], as it is illustrated in Fig. 21(b) and 22(c). The correction factor  $J/J_i$  is expressed as a ratio between two Bessel's functions,  $K_0$  (of zero order) and  $K_1$  (of the first order):  $J / J_i = K_0[(2/L(0)m)\sqrt{(mw+1)}] / \sqrt{(mw+1)} K_1[(2/L(0)m)\sqrt{(mw+1)}]$  where  $L(0)$  is the minority carrier length corresponding to the junction depth and  $w$  the thickness of the depleted region.

In Fig. 22 (b) is represented the generating reverse current density of a p-n junction with diffused gold calculated according our model as a function of the specific parameter of the gold diffusion profile  $\ln(1+mw)$ , where  $w$  represents the width of the depletion region, the very good agreement between our model and the experimental data allowing the extraction of the parameter  $m$  of the gold profile for the two conditions of the gold diffusion at the temperatures  $T = 900^\circ\text{C}$  and  $T = 950^\circ\text{C}$ .

We calculated also and reported the modifications of the forward current density in the  $p-n$  junctions fabricated by ion implantation where the generated defects are electrically active due to the local trapping of the metallic impurities within the implanted layer [62]. It was shown that the shape of the forward characteristic I-V of the  $p-n$  junction is not modified by the spatial distribution of the recombination centres, but the value of the forward current density is modified by a factor depending on the parameters of the their distribution profile [62].

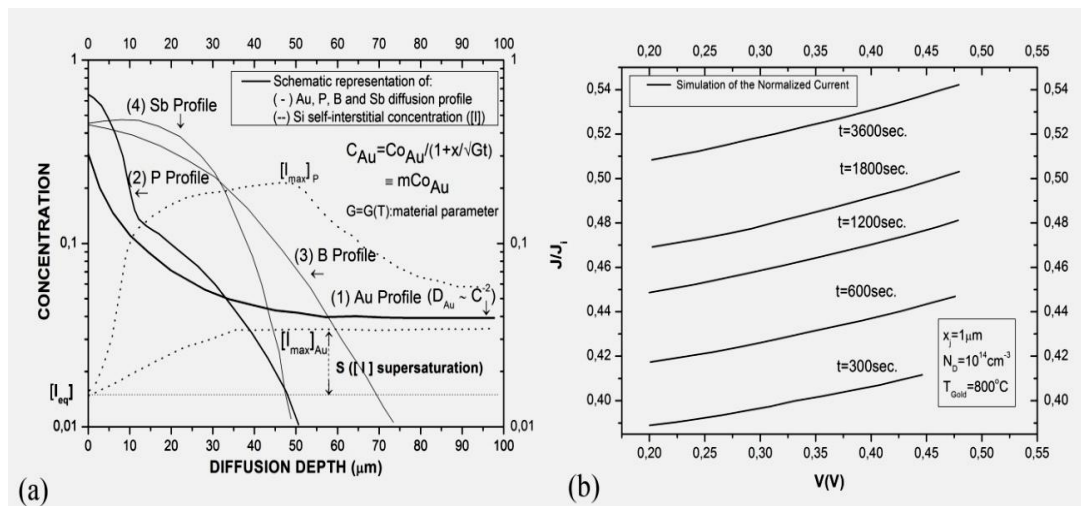


**Fig. 21.** (a) Au, P, B and Sb schematic representation profile and corresponding Si self-interstitial concentration. (b) Variation of  $J/J_i$  ( $V$ ) with Au diffusion time.

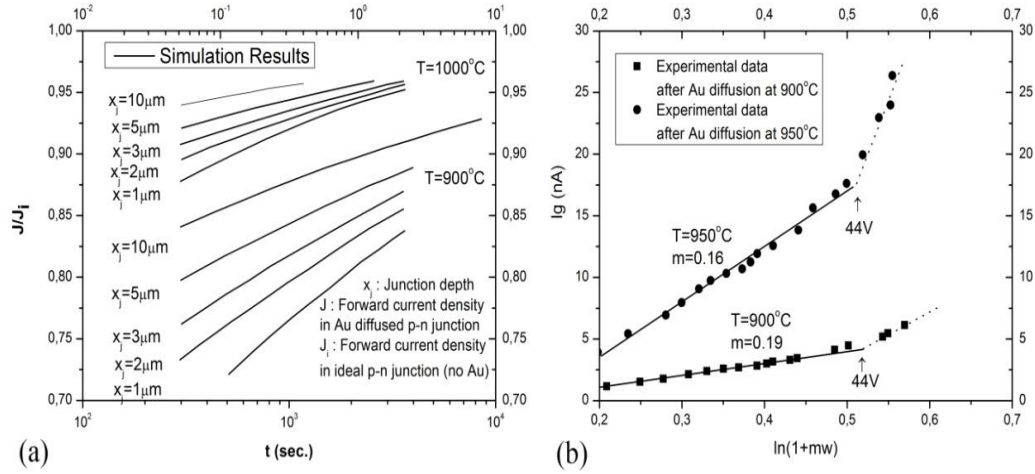


**Fig. 22.** (a) Variation of  $J/J_i$  with  $x_j$  and  $TAu$ . (b) Variation of the generation current density  $I_g$  with the parametric relation  $\ln(1+mw)$  in p-n diodes diffused with gold at  $900^\circ\text{C}$  and  $950^\circ\text{C}$  for 15 min, the arrow marking the start of the breakdown state.

In opposition to the previously described situation, the objective of the gettering process is to trap the metallic impurities in the highly doped layers, in order to increase the minority carrier life time in the electrically active silicon bulk regions and to improve consequently the efficiency of the photovoltaic cells or other sensitive devices. By a careful analysis of the diffusion profiles of P, B, Sb and As doping impurities with respect to that of Au in silicon and of the corresponding Si self-interstitial currents injected by the diffusion, we shown [61] (Fig. 8 (a)) that the self – interstitial current generated by P and B diffusion is favorable to enhance the transport and gettering of Au and Pt near the silicon surface, while As and Sb diffusion in silicon do not induce a similar transport and gettering process because their corresponding dominant diffusion mechanism is done by means of vacancies.

The interstitial current induces a drift of 3d metallic elements (cobalt group) near the surface, because the substitution component has a significant concentration only in the highly P doped layer. In highly B doped silicon, the 3d elements exhibit an increased solubility of their interstitial component and therefore the interaction with the Si self-interstitials is not an operative transport mechanism in that case.

Such accurate results were included in process simulators or in our patents dedicated to the fabrication technologies of various types of silicon devices as J-FET transistors, electroluminescent diodes, MESA power diodes, photovoltaic devices (solar cells), phototransistors, planar epitaxial diodes and integrated circuits [27-30, 46, 62-66].

## 5. Simulation and modelling of specific processes in silicon and polysilicon layers for membrane achievement

We started our researches on both the bulk and surface micromachining technology to optimize the specific processes for the fabrication of silicon membranes for capacitive pressure sensors for biomedical applications within the CASE European Project CASE [67]. In the bulk micromachining technology it is necessary to control the etching process on the highly boron doped silicon layers to control the final thickness of the membrane and also to diminish the internal stress induced by the mismatch into the silicon lattice [56]. The surface micromachining technology is based on the etching of the SiO<sub>2</sub> layers below the phosphorus doped polysilicon layers so that the optimization of the annealing process during the phosphorus diffusion in polysilicon is necessary to reduce or eliminate the internal stress [67].

### 5.1 Simulation of the etching process after the boron diffusion in silicon for the achievement of the silicon membranes by bulk micromachining technology

Our researches devoted to the silicon membrane achievement by bulk micromachining technology for the capacitive pressure sensors for biomedical applications within the frame of CASE European project [67], started from the observation that the specific boron profile redistributed after the implantation [68] or after thermo-chemical diffusion [69] in the bulk micromachining technology will determine a variation of the chemical etching rate  $R$  with respect to the rate  $R_i$  in weakly doped silicon in 10% KOH (LiOH, NaOH) or EDP (ethylene-diamine-pyrocatechol) solution at the etching temperature  $T_e = 60^\circ\text{C}$  for which  $a = 4$  and in 24% alkaline type solutions for which  $a=2$  in the relation  $R/R_i=1/[1+C/C_0]^{a-4/a}$  [70].

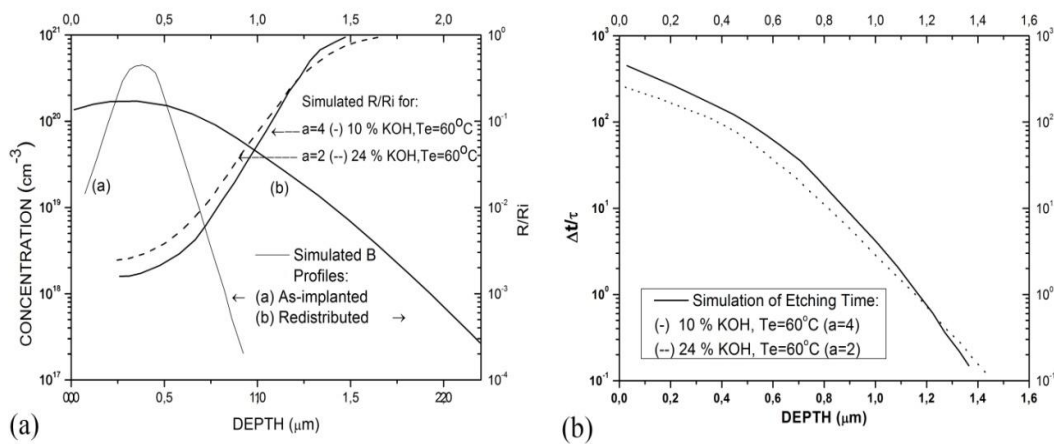


**Fig. 23.** (a) Variation of  $R/R_i$  with the depth of silicon layers doped by implantation.  
(b)  $\Delta t/\tau$  vs. depth during the etching of the implanted layer.

The results of our simulated boron doping profiles, chemical etching rate and corresponding etching time  $\Delta t$ , allowing a correct control of the etching process, are shown in Fig. 23 (a) and (b) for a boron implanted layer and in Fig. 24 (a) and (b) for a boron doped layer by diffusion from BN source [56, 69].

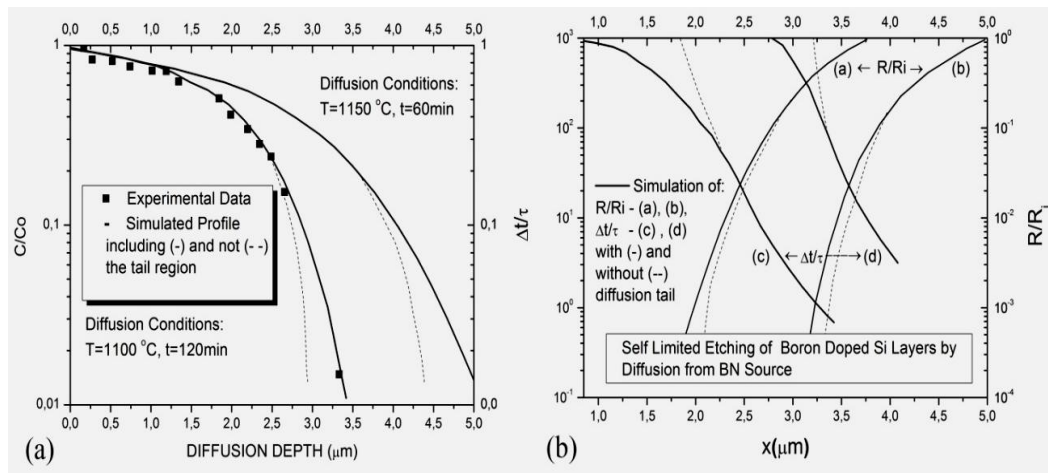


**Fig. 24.** (a) Variation with the depth of the boron diffusion profile with (full line) and without (dashed line) contribution in the intrinsic range. (b) Corresponding  $R/R_i$  and  $\Delta t/\tau$  vs. depth during the etching of the BN diffused layers as described in Fig. 24 (a).

## 5.2 Modelling of the doping – restricting process during the phosphorus diffusion on polysilicon layers for the achievement of the silicon membranes by surface micromachining technology

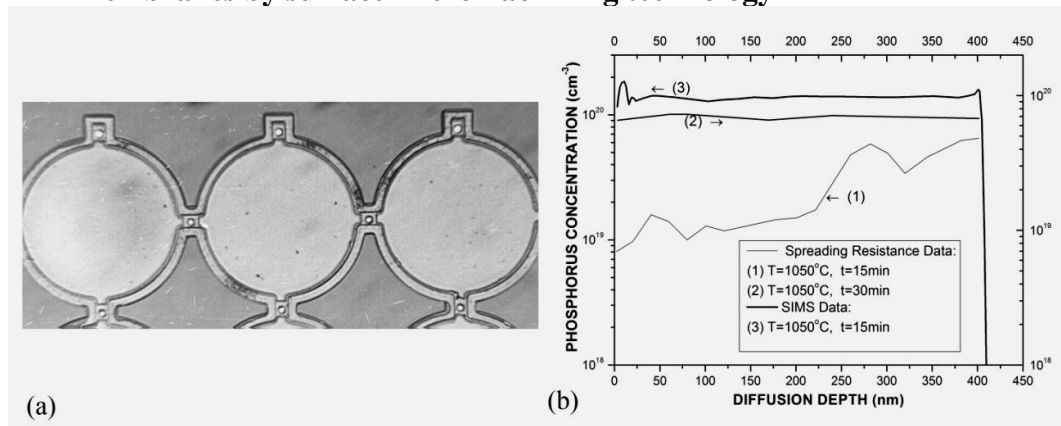


**Fig. 25.** (a). Capacitive sensor structure for biomedical applications fabricated by our micromachining technology. (b) SIMS and SRP phosphorus diffusion profiles showing the electrical activation of phosphorus atoms after diffusion.

The main objective of the researches to obtain silicon capacitive sensors by surface (polysilicon based) micromachining technology (Fig. 25 (a)) was to reduce or eliminate the internal stress or stress gradient induced by the atomic mismatch in the polysilicon layers doped by phosphorus diffusion and for this

purpose we used the secondary ion mass spectroscopy (SIMS) and spreading resistance profiling (SRP), correlated with cross-section electron transmission spectroscopy (XTEM) to analyse the structure of LP-CVD polysilicon after the deposition and after the diffusion steps (Fig. 25 (b)) [71].

We proposed a doping – restructuring model [72-75] of the polysilicon layers to explain the mechanism of the restructuring processes [76] as follows: the P diffusion in polysilicon and the oxidation during the P thermo-chemical process ( $\text{POCl}_3$ ) inject Si self-interstitials which determine an enhancement of the grain growth. During the growth, the surface of grain boundary decreases correspondingly and thereby the inactive P amount segregated there. The enhancement of grain growth determines an enhancement of P atom incorporation in the grains, so that their diffusion in Si bulk furthermore generates self- interstitial atoms which additionally contribute to the growth enhancement, in a continuously self-promoted doping-restructuring process. We proposed also a mechanism implying the atomic transport of the oxygen by means of the mobile SiO species to explain the degradation of the  $\text{SiO}_2$  layer during the phosphorus diffusion and the formation of the  $\text{SiO}_2$  precipitates near the  $\text{SiO}_2$ /Silicon interface [77], as it can be seen in Fig. 26 (b). These mechanisms well explains the restructuring of the initial columnar type structure (Fig. 26 (a)) to a large grain one (Fig.26 (b)) and the reduction/ elimination of the internal stress by applying the optimal conditions of drive-in diffusion process for the fabrication of the silicon membrane for the capacitive pressure sensors with biomedical applications [71].

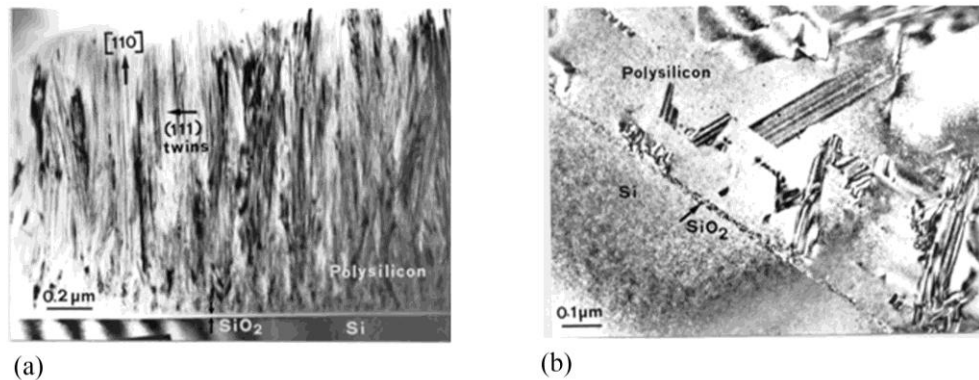


**Fig. 26.** (a). The columnar structure of the initial LP-CVD polysilicon layer.

(b) The large grain structure after the drive-in thermal process ( $T = 1030^\circ\text{C}$ , 20 min).

To obtain the full information on this technology we studied the polysilicon/ $\text{SiO}_2$ /silicon system under oxidizing conditions in oxygen gas (Fig. 27 (a)), and we explained the enhancement of the phosphorus diffusion coefficient in silicon observed by the fitting of our SIMS measurements on the diffusion profile with the default values used by SUPREM IV simulator by the excess of self -

interstitials atoms due to the dynamics of the reaction  $\text{Si} + \text{O} \rightarrow \text{SiO}$  and  $2 \text{SiO} \rightarrow 2 \text{Si} + \text{O}_2$ , where  $\text{SiO}$  is a mobile species in silicon [77, 78].

We studied also the formation of thin poly-SiC layers for micromechanical applications starting from the poly-Si layers implanted in multiple cycles with carbon with a dose in the range  $2.5\text{-}10 \times 10^{17} \text{ cm}^{-2}$  suitable that the solid solubility of the carbon concentration in silicon to be exceeded and energies in the range 40-120 keV and subsequent annealing at high temperature for a long time in order to assure the recrystallization process [79] (Fig. 26 (b)).

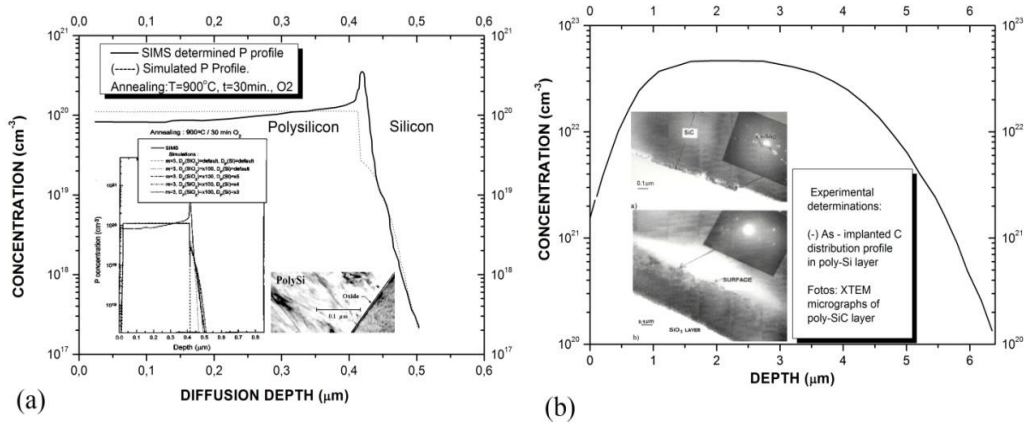


**Fig. 27.** (a). Simulated phosphorus diffusion profile (dashed line) in a Polysilicon/SiO<sub>2</sub>/Silicon system under oxidizing conditions at  $T = 900^\circ\text{C}$ ,  $t = 30 \text{ min}$  in oxygen gas compared with experimental SIMS profile (full line); the inserted photo is an XTEM micrograph of the analyzed system and the inserted graph represents various fitting values of the diffusion coefficient in silicon for a value of the segregation coefficient  $m = 3$ . (b) As implanted carbon profile in silicon; the inserted photo represents an XTEM micrograph of the carbon rich and poly-SiC formed region of the polysilicon layer.

The simulated profile was correlated with XTEM micrographs (inserted in Fig. 26 (b)), showing a very close relation between the poly-SiC formation on the high carbon concentration region of the implantation carbon profile and a carbon rich layer in the region of lower carbon concentration near the polysilicon external surface [79].

## 6. Conclusions

We proposed as non-electrical new profiling methods to determine the entire impurity concentration diffused in silicon, electrically active and not active, the spectrographic emission dosing for the determination of the total boron concentration profile and the spectrophotometric dosing method for the determination of the total phosphorus diffusion profile, showing that after the boron diffusion in silicon from a solid BN source the all quantity of boron is electrically active, while after the phosphorus diffusion from  $\text{POCl}_3$  liquid source a significant quantity of phosphorus atoms is electrically inactive.

We show by a careful analysis of the spread experimental data on *B* diffusion in silicon that the *B* diffusion coefficient *D* varies as the square root of the boron concentration ( $D \sim C^{1/2}$ ) during the diffusion from  $\text{BBr}_3$  source, suggesting that the Si self-interstitial atoms contribute to the diffusion mechanism, while during the diffusion from a BN source ( $D \sim C$ ) do not.

A complete set of analytical relations were deduced to adequately describe the boron diffusion profile in these cases, both on the extrinsic and intrinsic concentration range, as well as the interest material parameters like the boron diffused quantity as a function of the diffusion time, the surface concentration and surface diffusion coefficient as a function of the diffusion temperature, the sheet resistivity and the average conductivity of the doped layers, explicitly expressing the corrections which we applied to the fundamental curves currently used in the planar technology for the evaluation of the electrical conduction of the doped layers.

To simulate the phosphorus diffusion in silicon we solved a non-linear partial derivate equation system on the three regions of the profile, where  $D \sim C^2$ ,  $D \sim C^{-2}$  and  $D = \text{const.}$  respectively and we obtained explicit expression on each that region, adequately describing the phosphorus diffusion profile for the usual range of the diffusion temperature (800°C - 1100°C), well-fitting with experimental data.

B, P, Sb and As diffusion in silicon were adequately simulated under various conditions after the diffusion by using conventional (thermo-chemical) and non-conventional techniques (implantation and laser – assisted annealing, polysilicon sources, doped oxide) with direct application in the transistor and integrated circuit fabrication technologies.

Thus, we shown that the Sb diffusion from thermo-chemical procedure can be adequately simulated taking into account a variation  $D \sim C$  on the extrinsic range and  $D = \text{const.}$  on the intrinsic range and that the boron and arsenic diffusion from the polysilicon doped sources can be described considering a variation  $D \sim C^{1/2}$  and  $D \sim C$  respectively.

We simulated the temperature variation in silicon induced by a pulse laser both during the irradiation of the exposed silicon surface and after the stop of the irradiation process for values of the temperature not exceeding the melting silicon point.

The redistribution of boron, phosphorus and arsenic in silicon by a pulse ruby laser annealing during a melting and recrystallization process was simulated by a convenient procedure to avoid the extreme complications arising from the temperature and time dependence of the diffusion coefficient.

Moreover, by an adequate additional procedure we expressed the redistribution profile during the laser – assisted annealing of Sb both with and without impurity losses at the external silicon surface.

We calculated and analysed in detail the concentration profile after diffusion in a multilayer system with three and four components, showing that simplified solutions which can be reduced to the first terms only could adequately describe the impurity diffusion in silicon in some practical cases.

We calculated and analysed also the impurity diffusion profile after diffusion from doped layers distinguishing the behaviour of entirely protected and partially protected sources.

A particular interest was focused on Zn diffusion in GaAs as an application of the impurity diffusion from and through the multilayer systems, allowing proposing new diffusion techniques for the fabrication of the electroluminescence diodes.

Accurate profile experimental data obtained after the redistribution of the phosphorus and boron diffusion in silicon including the oxidation process shown the behaviour of these impurities near the silicon/SiO<sub>2</sub> interface and we calculated the recovery boron diffusion profile during the post-oxidation annealing with application in MOS fabrication technologies.

We deduced suitable approximations of the diffusion equation to describe adequately the boron redistribution during the post-implantation multisequential thermal processes, particularly for the modelling and optimization process of the buried diffusion source for the fabrication of the isolation walls of the integrated circuits according to one of our patent, during the chemical etching process before of the epitaxial growth, described by a moving boundary problem and during the epitaxial growth itself.

We also described adequately the diffusion during subsequent thermal process after the boron implantation to form the surface diffusion source, necessary to complete the isolation wall by the touching of the two diffusion fronts.

As the stress induced by the misfit between the atom impurity radius and the host atom radius could affect the properties of the semiconductor devices especially by the generation of the misfit dislocations in the electrically active microelectronic structures and the mechanical properties of the micromechanical elements realized by micromachining technologies, we calculated the stress induced after the boron implantation in silicon, showing that it could contribute to the recovery of the primary implantation defects and the significant reduction of the dislocation loop density especially after the multisequential thermal annealing.

We explicitly deduced in terms of technological control parameters (time and temperature) the conditions of the generation of misfit dislocations, both for boron

and phosphorus diffusion in silicon at high concentrations, offering a suitable model for the generation of the misfit dislocations during the boron diffusion in silicon related by the maximum gradient of the concentration in the silicon bulk. We applied the bevel angle selective etching (BASC) technique and the secondary ion mass spectrography (SIMS) method to compare our theoretical calculations with accurate suitable experimental data, which proved the proposed model.

We found also that after the boron diffusion in silicon from BN source followed by an oxidation annealing process useful for the fabrication of the micromechanical elements by the bulk micromachining technology the density of the misfit dislocation is reduced and localized near the maximum gradient of boron concentration, in agreement with our model.

The influence of Au diffusion on the forward and reverse I-V characteristic of a *p-n* junction was analytically expressed and we proposed a gettering contributing mechanism by self-interstitial injection to explain the behaviour of Au, Pt and other metallic impurities in silicon.

We calculated also the influence on the forward I-V characteristic of the electrically active defects after the boron implantation in silicon.

These results on the impurity diffusion in silicon permitted innovative solutions included in fabrication patents and process simulators.

The optimization of the polysilicon drive-in processing by a doping – restructuring model and the simulation of etching process of the boron doped layer were successfully applied for the membrane achievement for the capacitive pressure sensors fabricated by surface and bulk micromachining technology.

We successfully extended our researches on the simulation of the phosphorus diffusion in silicon during the oxidation process from the polysilicon layers finding the correct fitting parameters used in SUPREM IV simulator and the formation of poly-SiC layers by carbon multisequential implantation and subsequent annealing for micromechanical applications.

Taking into account our presented results and future developments, we plan to prepare a Romanian simulator for microfabrication and micromachining technological processes.

### **Acknowledgement**

The author gratefully thanks to Dr. Constantin Bulucea, Honor Member of the Romanian Academy for his contribution to his professional trajectory and for his recommendation. He gratefully thanks to Prof. Dr. H. Richter (Frankfurt Institute of Semiconductor Physics), Ch. Lontos (University of Athens) for their collaboration and recommendations.

The author gratefully thanks to Prof. Dr. Paul Sterian and Dr. Cornel Cobianu, members of the Academy of Romanian Scientists, for their support and recommendation. He also thanks to Prof. Dr. Mircea Bodea and to all members of the Information Science and Technology of the Academy of the Romanian Scientists for their support.

The author gratefully thanks to Lord-Chaldran Professor Richard B. Fair (Duke University) and Ulrich Gösele (Max Planck Institute of Microstructure Physics) for their continuous appreciations.

He faithfully thanks to his exemplar parents, Professors Emanoil and Florica Gaiseanu and to his family, Maria, Florin, Adrian and Ana Maria Gaiseanu for their infinite patience and support.

## REFERENCES

- [1] C. Bulucea, "Planar low power transistors with silicon (I). Constructive parameters and bulk phenomena", *E.E.A. Automatics and Electronics*, vol. 13, No 1, (1969), pages 32-38.
- [2] D.J. Fisher, "Diffusion in Silicon - 10 Years of Researches", *Defect and Diffusion Forum, Scitec Publications*, vol. 153-155, (1997), pages 1-560.
- [3] P. Pichler, *Intrinsic Point Defects, Impurities and Their Diffusion in Silicon*, Computational Microelectronics, 2004, pp. 331-467.
- [4] F. Gaiseanu, V. Loghin, N. Kozma, M. Badila, "Determination of the shallow diffusion profiles of boron and phosphorus in silicon", *E.E.A. Automatics and Electronics*, vol. 23, No 1, (1979), pages 40-44.
- [5] F. Gaiseanu, V. Loghin, I. Burlacel, "Anomalous Boron Profile in Silicon after Diffusion from BN Source by H<sub>2</sub> Injection", *Revue Roumaine de Physique*, vol. 28, No 7, (1983), pages 625-630.
- [6] F. Gaiseanu, "Boron Diffusion Profile in Silicon and Data Analysis", *Journal of the Electrochemical Society*, vol. 132, No 9, (1985), pages 2287-2289.
- [7] F. Gaiseanu, "On the Diffusion Profile of Boron in Silicon at High Concentrations", *Phys. Stat. Sol., (a)*, vol. 77, (1983), pages K59-K61.
- [8] R.B. Fair, "Boron diffusion in silicon-concentration and orientation dependence, background effects, and profile estimation", *J. Electrochem. Soc.*, vol. 122, No 6, (1975), pages 800-805.
- [9] F. Gaiseanu, I. Dima, "Diffusion Coefficient of Boron in Silicon at High Concentrations", *Rev. Roum. Phys.*, vol. 34, No 4, (1989), pages 437-440.
- [10] S.F. Guo, W.S. Chen, "A Model for Boron Deposition in Silicon Using a BBr<sub>3</sub> Source", *J. Electrochem. Soc.*, vol. 129, No 7, (1982), pages 1592 - 1596.
- [11] F. Gaiseanu, "Progresses Related to the Study of the Boron Diffusion in Silicon", *Rev. Roum. Phys.*, vol. 32, (1987), pages 1067 - 1075.
- [12] P. Negrini, A. Ravaglia, S. Solmi, "Boron Predeposition in Silicon Using BBr<sub>3</sub>", *J. Electrochem. Soc.*, vol. 125, No 4, (1978), pages 609 - 613.
- [13] F. Gaiseanu, "Resistivity of the Silicon Layers Doped with Boron by Using a BBr<sub>3</sub> Source", *Meeting of the Electrochem. Soc., Toronto (Canada), May 15-17, 1985 and J. Electrochem. Soc.*, vol.132, (1985), Abstract 113C.
- [14] F. Gaiseanu, "Average Conductivity of Silicon Layers Doped by Boron Diffusion from an Infinite Source", *J. Electrochem. Soc.*, vol. 132, (1985), Abstract 445C.
- [15] D. Antoniadis, A. Gonzalez, R. Dutton, "Boron in Near - Intrinsic <100> and <111> Silicon under Inert and Oxidizing ambient - Diffusion and Segregation", *J. Electrochem. Soc.*, vol. 125, (1978), pages 813-819.
- [16] F. Gaiseanu, "Advances in the Modelling of the Impurity Diffusion in Semiconductors", *Rev. Roum. Phys.*, vol. 37, No 5, (1992), pages 509-520.

- [17] U. Gösele, T. Tan, "The Nature of Point Defects and Their Influence on Diffusion Processes in Silicon at High Temperatures", *Mat. Res. Soc. Symp. Proc.*, vol. 14, (1983), pages 145-159.
- [18] F. Morehead, R. Lever, "Enhanced "Tail" Diffusion of Phosphorus and Boron in Silicon: Self-Interstitial Phenomena", *Appl. Phys. Lett.*, vol. 48, No 2, (1986), pages 151-153.
- [19] R. Fair, J.C.Tsai, "Quantitative Model for the Diffusion in Silicon and the Emitter Dip Effect", *J. Electrochem. Soc.*, vol. 133, No 7, (1977), pages 1107-1117.
- [20] F. Gaiseanu, "Analytical Model Simulating the Shallow Phosphorus Diffusion in Silicon", *J. Electrochem. Soc.*, vol. 133, page 329 C, and in the Special Volume of Symposium *Process Physics and Modeling in the Semiconductor Technology*, edited by G. Srinivasan, D. Antoniadis, J. Plummer, (1988), pages 86-97.
- [21] F. Gaiseanu, "Analytical Model Simulating the Phosphorus Diffusion in Silicon", *Rev. Roum. Phys.*, vol. 35, No 1, (1990), pages 65-73.
- [22] F. Pintchovski, P. Tobin, M. Kottke, J. Price, "Antimony Diffusion in Silicon: Effects on Ambient Gas and Time", *J. Electrochem. Soc.*, vol. 131, No 8, (1984), pages 1875-1883.
- [23] F. Gaiseanu, C. Postolache, "Antimony Diffusion Profile in Silicon: Analysis and Modelling", *J. Electrochem. Soc.*, vol. 133, (1986), Abstract 445C.
- [24] F. Gaiseanu, C. Postolache, "Analytical Modeling of Antimony Diffusion in Silicon", *Electrochem. Soc. Meet.*, Phoenix, Arizona, Oct. 13-18<sup>th</sup>, (1991).
- [25] F. Gaiseanu, "Analytical Approach to Impurity Redistribution During Post-Oxidation Annealing of Silicon", *Rev. Roum. Phys.*, vol. 34, No 1, (1989), pages 123-129.
- [26] F. Gaiseanu, M. Badila, C. Postolache, I. Dima, "On the Antimony Redistribution in Silicon During the Post-Implantation Annealing", *Revue Roumaine de Physique*, vol. 32, No 4, (1987), pages 429-433 (results included by request in SUPREM and PREDICT simulator).
- [27] C. Postolache, F. Gaiseanu, C. Popescu, "Isolation Technique of the Components from the Monolithic Integrated Circuit Structure", *Romanian Patent* N° 96 889, (1988).
- [28] F. Gaiseanu, M. Badila, I. Ghita, "Procedure for the Fabrication for the Field Effect Transistors with Gate with Integrated Junction", *Romanian Patent* N° 81 821, (1983).
- [29] C. Postolache, F. Gaiseanu, D. Serghi, "Procedure for the Structure Fabrication of the Junction Field Effect Transistor", *Romanian Patent*, N° 96 766, (1988).
- [30] C. Postolache, F. Gaiseanu, "Procedure for the Monolithic Integration of the Junction Field Effect Transistor", *Romanian Patent*, N° 96 767, (1988).
- [31] F. Gaiseanu, M. Badila, "Simulation of the Boron Diffusion Process after the Implantation in Silicon", Prague, Czechoslovakia, *Proceeding of the Microelectronic Conference*, Sept. 4-6<sup>th</sup>, vol. 1, (1984), pages 63-66.
- [32] F. Gaiseanu, "Analytical Approximations of the Impurity Redistribution During Post – Implantation Annealing", *Revue Roumaine de Sciences Techniques, Electronique et Energetique*, vol. 37, No 2, (1992), pages 185-199.
- [33] C. Postolache, F. Gaiseanu, R. Mazilu, "Redistribution of the Buried Source, Modeling and Comparative Analysis", *E.E.A. Automatics and Electronics*, vol. 34, No 3, (1990), pages 77-85.

- [34] W. White, C. Christie, W. Appleton, S. Wilson, P. Pronko, C. Magee, "Redistribution of Dopants in Ion-Implanted Silicon by Pulsed-Laser Annealing", *Appl. Phys. Lett.* Vol. 33, (1978), pages 662 – 664.
- [35] F. Gaiseanu, "Laser Induced Temperature in Solids: Analytical Results", *Revue Roumaine de Sciences Techniques, Electronique et Energetique*, vol. 35, No 4, (1990), pages 495-502.
- [36] F. Gaiseanu, M., Bazu, L., Galateanu, "Impurity Redistribution During Post-Implantation Laser Annealing: Analytical Evaluation", *Revue Roumaine de Physique*, vol.35, No3, (1990), pages 283-288.
- [37] F.Gaiseanu, L. Galateanu, "Analytical Modeling of the Redistribution During Laser Annealing of the Group V Impurities Implanted in Silicon", *Second International Conference on Solid State and Integrated Circuit Technology*, Organized by Berkley University of California in Beijing, China, Oct. 22-28<sup>th</sup>, (1989).
- [38] F. Gaiseanu, "Advances in the Modeling of the Impurity Diffusion in Silicon", *Revue Roumaine de Physique*, vol. 37, No 5, (1992), pages 509-520.
- [39] F. Gaiseanu, "Rapid Heating Multilayer Structure for Industrial Application", *JBC Industries, Private Communication*, Barcelona, (2008), pages 1-30.
- [40] F. Gaiseanu, "An Analytical Model for Boron and Arsenic Diffusion in Silicon from Polysilicon Sources", *Electrochem. Soc. Meeting*, Montreal, Canada, May 6-11, *J. Electrochem. Soc.*, vol. 137, 1014RNP, (1990), page 287C.
- [41] V. Probst, H. Bohm, H. Schaber, H. Oppoler, I. Weitzel, "Analysis of Polysilicon Diffusion Sources", *J. Electrochem. Soc.*, vol. 35, No 3, (1991), pages 37-39.
- [42] F. Gaiseanu, "Analytical Modeling of the Boron and Arsenic from Polysilicon Sources Doped by Ion Implantation", *E.E.A. Automatics and Electronics*, vol. 35, No 4, (1991), pages 37-39.
- [43] F. Gaiseanu, "Analytical Model of the Impurity Diffusion From an Infinite Source Through a Multilayer System into a Semi-Infinite Adjacent Solid", *Revue Roumaine de Science Technique, Electronique et Energetique*, vol. 35, No 2, (1990), pages 253-264.
- [44] F. Gaiseanu, "Modeling of the Impurity Diffusion from Protected Sources", *J. Electrochem. Soc.*, vol. 137, 866RNP, (1990), page 531C.
- [45] F. Gaiseanu, "Impurity Diffusion in Semiconductors from Multi-Layer Source Systems", *Revue Roumaine de Science Technique, Electronique et Energetique*, vol. 36, No 4, (1991), pages 481-500.
- [46] I. Burlacel, C. Postolache, A. Alamariu, V. Paun, F. Gaiseanu, "Procedure for the Local Source Deposition for Zn Doping of the Semiconductor Wafers", *Romanian Patent* N° 91.160, (1987).
- [47] F. Gaiseanu, H. Ciubotariu, A. Necula, M., Moroseanu, "Zn Diffusion on GaAs through SiO<sub>2</sub> Layers", *E.E.A. Automatics and Electronics*, vol. 26, No 2, (1982), pages 63-67.
- [48] D. Sachelarie, C. Postolache, F. Gaiseanu, "Diffusion Pipes in *pn*p Switching Transistors", *Studies and Researches of Physics*, vol. 24, No 4, (1974), pages 327-338.

- [49] D. Sachelarie, M. Dragan, M. Sachelarie, F. Gaiseanu, "Recombination Current from the Depletion Region of the  $p$ - $n$  Junctions with Gold, Forwardly Polarized", *E.E.A. Automatics and Electronics*, vol. 21, No 3, **1977**, pages 95-99.
- [50] D. Sachelarie, M. Bazu, M. Sachelarie, F. Gaiseanu, D. Lungu, "Charge State of the Gold Energetic Levels from the Space Charge Region of the  $p$ - $n$  Junctions with Silicon", *E.E.A. Automatics and Electronics* vol. 20, No 3, (**1976**), pages 114-119.
- [51] F. Gaiseanu, L. Galateanu, M. Bazu, "Dislocations in (111) Oriented Silicon Revealed by Preferential Chemical Etching", *Proc. of Gettering and Defect Engineering in Semiconductor Technology* (GADEST), First International Autumn School, Oct. 8-18<sup>th</sup>, Garzau (Germany), edited by H. Richter, vol. 1, (1985), pages 207-210.
- [52] F. Gaiseanu, L. Galateanu, M. Bazu, R. Plugaru, "Simulation of the Misfit Elastic Stress Induced by Implanted Impurities in Semiconductor Wafers", *Proc. of the 7- th Mediterranean Electrotechnical Conf.*, (MELECON) Antalya, Turkey, Apr. 12-14<sup>th</sup>, vol. 2, (**1994**), pages 599-600.
- [53] R. Plugaru, F. Gaiseanu, M. Bazu, L. Nistor, "Analysis of the Defects Induced by Boron Implantation in Silicon after Sequential Annealing Processes", *Proc. of the 7- th Mediterranean Electrotechnical Conf.*, Antalya, Turkey, Apr. 12-14<sup>th</sup>, vol. 2, (**1994**), pages 597-598.
- [54] F. Gaiseanu, "Critical Conditions for the Generation of the Misfit Dislocations During the Boron Diffusion in Silicon", *Solid State Phenomena*, vol. 47&48, (**1995**), pages 223-229.
- [55] F. Gaiseanu, G. Kissinger, D. Kruger, H. Richter, "Analysis of the Generation of the Misfit Dislocations During the Boron Prediffusion in Silicon", *Proc. SPIE (The International Society for Optical Engineering) 3507, Process, Equipment, and Materials Control in Integrated Circuit Manufacturing IV*, Santa Clara, California, Sept. 23-24<sup>th</sup>, (**1998**), pages 281-289.
- [56] F. Gaiseanu, J. Esteve, G. Kissinger, D. Krüger, "Diffusion Induced Dislocations in Highly Boron-Doped Silicon Layers Used for Micromachining Applications", *Proc. of SPIE (The International Society for Optical Engineering) 3511, Micromachining and Microfabrication Process Technology IV*, Santa Clara, California, Sept. 20-22<sup>nd</sup>, (**1998**), pages 88-96.
- [57] F. Gaiseanu, "Analytical Model to Calculate the Conditions of Phosphorus Induced Misfit Dislocations in Silicon", *Rev. Roum. Sci. Tech.*, vol. 38, No 1, (**1993**), pages 107-113.
- [58] F. Gaiseanu, R. Plugaru, M. Bazu, O. Buiu, "Generation of the Induced Misfit Dislocations During the Phosphorus Diffusion in Silicon: Analytical Determination, Solid State Phenomena", vol. 32&33, (**1985**), pages 93-98.
- [59] R. Fair, "Quantified Conditions for the Emitter-Misfit Dislocation Formation in Silicon", *Journal of the Electrochemical Society*, vol. 123, No 8, (**1978**), pages 923-926.
- [60] F. Gaiseanu, M. Sachelarie, D. Sachelarie J. Esteve, "Analytical Modeling of the Gold Diffusion Induced Modification of the Forward Current Density Through the  $p$ - $n$  Junctions", *Solid State Phenomena*, vol. 37-38, (**1997**), pages 525-530.
- [61] F. Gaiseanu, W. Schröter, "Contribution of Diffusion Interstitial Injection to the Gettering of Metallic Impurities in Silicon", *J. Electrochem. Soc.*, vol. 143, No 1, (**1996**), pages 361-362.
- [62] F. Gaiseanu, "Influence of the Spatially Distributed, Electrically Active, Implantation Induced Defects on the Diffusion Current Through the  $p^+$ - $n$  Junctions", *Proc. of GADEST (Gettering and defect Engineering in the semiconductor technology), First International Autumn School*, Oct. 8-18<sup>th</sup>, Garzau (Germany), edited by H. Richter, (**1985**), pages 236-238.

- [63] F. Gaiseanu, C. Postolache, "Procedure for the Local Gettering of the Semiconductor Structures with Silicon", *Romanian Patent* N° 100 284, (1989).
- [64] C. Postolache, A. Rusu, F. Gaiseanu, "Procedure for the Fabrication of the High Power and High Breakdown Voltage", *Romanian Patent* N° 102 481, (1989).
- [65] GĂISEANU, F., POSTOLACHE, C., *Procedure for the Fabrication of Planar – Epitaxial Diode Structure for High Breakdown Voltage*, Romanian Patent N° 102 270, 1988.
- [66] C. Postolache, F. Gaiseanu, "Procedure for the Fabrication of Buried Sources Isolated with Respect to the Substrate", *Romanian Patent* N° 103 681, 1988.
- [67] a) F. Gaiseanu, C. Postolache, "Procedure for the Gettering and local Passivation of the Diode silicon Structures Fabricated by MESA Technique", Romanian Patent N° 103 860, (1988).  
b) F. Gaiseanu, "Project CASE, Inco-Copernicus 960136, WP4 Material Characterization", 2<sup>nd</sup> *Technical Report*, (1998), pages 43-91.
- [68] F. Gaiseanu, C. Cobianu, D. Dascalu, "Dependence of the Chemical Etch Rate and Etch Time of Silicon on the Post-Implanted Diffusion Depth: Application for Membrane Achievement", *Journal of Material Science Letters*, vol. 12, (1993), pages 1652-1653.
- [69] F. Gaiseanu, D. Tsoukalas, J. Esteve, C. Postolache, D. Goustouridis, E. Tsoi, "Chemical Etching Control During the Self-limitation Process by Boron Diffusion in Silicon: Analytical Results", *Proceedings of CAS' 97, International Semiconductor Conference*, Sinaia (Romania), Oct. 7-11, vol.1, (1997), pages 247-250.
- [70] H. Seidel, L. Csepregi, A. Heuberger, H. Baumgartel, "Anisotropic Etching of Crystalline Silicon in Alkaline Solutions - Orientation Dependence and Behavior of Passivation Layers", *J. Electrochem. Soc.*, vol. 137, (1990), pages 3612-3626.
- [71] F. Gaiseanu, C. Postolache, D. Dascalu, J. Esteve, D. Tsoukalas, A. Badoiu, E. Vasile, "Material and Device Characterization for Process Optimization of the Capacitive Pressure Sensors for Biomedical Application Achieved by Surface Micromachining Technology", *Romanian Journal of Information Science and Technology*, vol. 1, No 1, (1998), pages 85-104.
- [72] F. Gaiseanu, C. Dimitriadis, J. Stoemenos, C. Postolache, C. Angelis, "Structural Modifications of the Thick Polysilicon Layers on Silicon During Phosphorus Contributing Mechanisms", Best Paper Award, *Proceedings of CAS'96, International Semiconductor Conference*, Sinaia (Romania), Oct. 9-12, vol. 1, (1996), pages 61- 64.
- [73] F. Gaiseanu, C. Dimitriadis, J. Stoemenos, C. Dimitriadis, C. Postolache, H. RICHTER, W. Schroter, M. Seibt, "A Contributing Mechanism to the Doping – Restructuring Process During Phosphorus Diffusion in Polysilicon Layers", *Meeting of the Electrochemical Society*, San Antonio, Oct. 5<sup>th</sup> – 10<sup>th</sup>, (1996).
- [74] F. Gaiseanu, C. Dimitriadis, J. Stoemenos, C. Postolache, C. Angelis, D. Tsoukalas, D. Kruger, E. Tsoi, "Restructuring – Doping Process near the Polysilicon/SiO<sub>2</sub> Interface on Silicon During the Phosphorus Diffusion", *Proc. of the Electrochem. Soc. Meeting, EUROCVI – 11 SYMPHOSIUM*, Edited by Claude Bernard, Paris, Aug. 31 – Sept. 5<sup>th</sup>, (1997), pages 1289-1296.
- [75] F. Gaiseanu, C. Postolache, D. Dascalu, J. Esteve, D., Tsoukalas, R. Jachowicz, A. Badoiu, E. Vasile, "Material Characterization of the Capacitive Pressure Sensors for Biomedical Application Fabricated by Surface Micromachining Technology", *EUROSENSORS XII Conference*, vol. 1, organized by Prof. J.E. Brignell in Southampton, Sept. 13-16, (1998).

[76] F. Gaiseanu, J. Esteve, C. Cane, A. Perez-Rodriguez, J. Morante, C. Serre, "Doping and Structural Properties of the Phosphorus-Doped Polysilicon Layers for Micromechanical Applications", *Proc. SPIE Micromachining and Microfabrication Process Technology V*, Sept. 20-22<sup>nd</sup>, Santa Clara, California, Volume 3874 edited by J. Smith and J.M. Karam, Sept. 13-16, (1999), pages 412-422.

[77] F. Gaiseanu, D. Tsoukalas, C. Londos, J. Stoemenos, C. Dimitriadis, J. Esteve, C. Postolache, M. Bercu, "Oxygen Related Transport Phenomena Near the Polysilicon/SiO<sub>2</sub> Interface on Silicon During Phosphorus Diffusion", *Romanian Journal of Physics*, vol. 43, No 7-8, (1998), pages 593-601.

[78] F. Gaiseanu, D. Tsamis, D. Tsoukalas, D. Kruger, C. Tsamis, J. Stoemenos, C. Dimitriadis, H. Vassilakis, "Analysis of Phosphorus Diffusion in the Polysilicon/Oxide/Silicon System under Oxidizing Conditions for Profile Simulation", *Meeting of the Electrochem. Soc.*, Boston, Oct. 9-14, (1998).

[79] F. Gaiseanu, J. Rodriguez, M. Mora, "Structure of the Poly-SiC Formed by High Dose Carbon Implantation in Poly-Si Layers", *Meeting of the Electrochem. Soc., Material Science Symposium*, Boston, Oct. 20-24<sup>th</sup>, (2000).